

The fate of Schwarzschild–de Sitter black holes: nonequilibrium evaporation

Damien A. Easson

*Department of Physics & Beyond Center for Fundamental Concepts in Science,
Arizona State University, Tempe, AZ 85287-1504, USA*

Abstract

We present a fully analytic treatment of Schwarzschild–de Sitter (SdS) black-hole evaporation in two-dimensional dilaton gravity with anomaly-induced backreaction. Starting from the spherical reduction of four-dimensional Einstein gravity with a cosmological constant, we construct an exactly solvable 2D model that captures the full causal and thermodynamic structure of the SdS static patch, including both black-hole and cosmological horizons. Incorporating the trace anomaly of N conformal matter fields via the Polyakov action, we determine the evolution of the black-hole mass and geometry in the Unruh–de Sitter state, track the steady nonequilibrium Hawking flux, and compute local thermodynamic observables for static observers. The conserved Killing energy flux drives an irreversible heat current from the black hole to the cosmological horizon whenever their surface gravities differ, ensuring monotonic entropy growth and satisfaction of the generalized second law. We prove that $\kappa_b > \kappa_c$ throughout the physical static patch, so the only zero-flux configuration is the Nariai limit where the horizons coincide. Extending the framework to the quantum-information regime, we construct a thermo-controlled estimate of the Page curve and show how quantum extremal surfaces and entanglement islands emerge naturally within the anomaly-induced steady state. These results constitute a fully analytic, backreacted solution for SdS evaporation that unifies semiclassical thermodynamics and information flow in a cosmological setting, thereby elucidating the ultimate fate of evaporating black holes in de Sitter space.

CONTENTS

I. Introduction	4
II. From 4D Schwarzschild–de Sitter to 2D dilaton gravity	6
A. Weyl frame and SdS solution	6
III. Semiclassical trace–anomaly backreaction	7
A. Conserved flux and mass–loss law	8
B. Local temperatures and Tolman redshift	10
IV. Evaporation Dynamics and Mass Evolution	11
A. Flux, equilibrium and evolution timescales	12
V. Quasi-stationary geometry from localized Polyakov action	13
A. Localized action and semiclassical equations	13
B. Solution structure and horizon regularity	14
VI. Equilibrium Configurations and Stability	15
A. The Nariai limit and zero–flux equilibrium	16
B. Phase diagram	17
VII. Observer-dependent thermodynamics	18
A. Local temperatures and steady flux	19
B. Near-horizon behavior and regularity	20
C. Detector response	20
VIII. Entropy flow and the generalized second law	21
A. Entropy balance and first-law structure	21
1. Flux balance and horizon Clausius relations	21
2. Generalized second law	22
IX. Quantum Extremal Surfaces and Entanglement Islands	22
A. Generalized entropy and QES conditions	23
B. Islands in the static patch	24
1. Entanglement structure	24

2. Cosmological counterpart	25
C. A thermo-controlled Page-curve estimate	26
1. Refined Page condition	27
 X. Conclusions	30
A. Main conclusions	30
B. Future directions	31
 Acknowledgments	32
 A. Exact quadrature reduction and the static momentum constraint	33
1. Preliminaries in static gauge	33
2. First integrals	34
3. Static momentum constraint and a no-go for exact static flux	34
4. Quadratures and horizon regularity (static, zero-flux case)	35
5. Dimensional-reduction anomaly	36
 B. Adiabatic evolution in Eddington–Finkelstein gauge and the mass–loss law	37
1. EF ansatz and basic identities	37
2. Mixed Einstein equation and state flux	38
3. Mass function (Casimir) balance and $\dot{M} = -\mathcal{J}$	38
 C. Nariai limit in the two–dimensional reduction	39
1. Near-horizon scaling and coordinates	40
2. Two-dimensional Nariai geometry	40
3. Interpretation in the 2D dilaton theory	41
 D. Curvature scalar and horizon regularity	41
1. Ricci scalar in static (or EF) gauge	42
2. Finiteness at the horizons	42
3. Classical limit and backreaction corrections	43
 References	43

I. INTRODUCTION

The discovery by Bekenstein and Hawking that black holes radiate thermally and carry entropy revolutionized our understanding of gravity and thermodynamics, revealing that classical event horizons are inherently quantum objects [1–5]. In an accelerating de Sitter universe, black holes coexist with a cosmological horizon, each characterized by its own surface gravity and associated temperature. Unlike asymptotically flat black holes, this dual-horizon structure places the system in intrinsic nonequilibrium: both horizons radiate, but generally at different temperatures. Despite significant progress, a complete understanding of how black holes evaporate in de Sitter space and how the second law of thermodynamics is realized in such spacetimes remains a fundamental open problem.

The two-dimensional trace-anomaly method, pioneered by Polyakov [6] and developed in many subsequent works [7–11], provides a powerful framework for semiclassical gravity. In this approach, the backreaction of N conformal matter fields is encoded in an anomaly-induced effective action that captures quantum stress–energy effects in a geometrically transparent form, allowing controlled calculations of Hawking flux and backreaction in both asymptotically flat and cosmological settings (see, e.g., [9, 12–14]). Yet an analytic, self-consistent treatment of Schwarzschild–de Sitter (SdS) evaporation that simultaneously tracks both horizons, real-time mass evolution, and the thermodynamic response of local observers has yet to be achieved.

Recent studies have analyzed SdS and Kerr–de Sitter evaporation in four dimensions [15–18], incorporating greybody factors and mode-by-mode fluxes for scalar, electromagnetic, and gravitational perturbations. These works demonstrate consistency with the generalized second law but rely on numerical computation and do not yield closed-form expressions for fluxes, mass evolution, or local thermodynamic quantities. A complementary, fully analytic framework can therefore provide valuable geometric insight and a benchmark for these numerical analyses.

Here we construct such a platform using two-dimensional dilaton gravity with anomaly-induced backreaction. Starting from the spherical reduction of four-dimensional Einstein gravity with a cosmological constant, we obtain an exactly solvable two-dimensional model that reproduces the causal and thermodynamic structure of the SdS static patch. Incorporating the Polyakov effective action, we determine the anomaly-induced energy flux, derive

the evolution equation for the black-hole mass, and compute local temperatures, energy densities, and fluxes measured by static observers. In two dimensions, the anomaly-induced action captures the complete semiclassical dynamics of the s -wave sector [19], enabling a self-consistent treatment of backreaction.

The resulting system realizes a nonequilibrium steady state with constant energy flow from the hotter black hole to the cooler cosmological horizon. The mass-loss law admits a single equilibrium point, the Nariai configuration, where the horizons coincide and their surface gravities vanish. We construct the (M, Λ) phase diagram, identify its fixed points, and verify that the generalized second law is satisfied throughout the evaporation process.

Building on this thermodynamic foundation, we develop a thermo-controlled estimate of the Page curve and show how quantum extremal surfaces and entanglement islands emerge naturally in the Unruh–de Sitter state. This connects the nonequilibrium thermodynamics of de Sitter black holes with their underlying information flow, providing a new analytic bridge between horizon thermodynamics and the island paradigm in a cosmological context.

These results yield a fully analytic, backreacted description of Schwarzschild–de Sitter evaporation that unifies semiclassical thermodynamics and information dynamics within a single, exactly solvable framework. The construction captures flux conservation, entropy balance, Page-like behavior, and endpoint classification under analytic control, complementing prior numerical analyses and offering exact geometric insight into evaporation, entropy production, and information recovery in multi-horizon spacetimes. Moreover, the methods developed here extend naturally to charged or regular (nonsingular) black holes [20–27], providing a foundation for future studies of quantum extremal surfaces and information flow in dynamical backgrounds.

The remainder of this paper is organized as follows. Section II reviews the spherical reduction to two-dimensional dilaton gravity. Section III develops the semiclassical anomaly framework and the mass-loss law. Section IV analyzes evaporation dynamics, Section V the quasi-stationary geometry, and Section VI equilibrium and stability. Sections VII and VIII discuss observer thermodynamics and the generalized second law, followed by Section IX on quantum extremal surfaces, entanglement islands, and the Page curve. Technical derivations appear in Appendices A–D.

II. FROM 4D SCHWARZSCHILD–DE SITTER TO 2D DILATON GRAVITY

To begin, for completeness we briefly summarize the spherical reduction of four-dimensional Einstein–Hilbert (EH) gravity with cosmological constant to its two-dimensional dilaton form, following standard treatments and exhibit the Schwarzschild–de Sitter (SdS) solution in the reduced theory.¹

Starting from the 4D EH action with cosmological constant,

$$S_4 = \frac{1}{16\pi G_4} \int d^4x \sqrt{-g^{(4)}} (R^{(4)} - 2\Lambda) , \quad (1)$$

we assume a spherically symmetric metric ansatz

$$ds_{(4)}^2 = g_{ab}(x) dx^a dx^b + r(x)^2 d\Omega_2^2, \quad a, b \in \{0, 1\}, \quad (2)$$

and define the dilaton as the area variable,

$$X(x) := r(x)^2. \quad (3)$$

The four-dimensional Ricci scalar decomposes (up to total derivatives) as

$$R^{(4)} = R - \frac{2}{X} \nabla^2 X + \frac{1}{2X^2} (\nabla X)^2 + \frac{2}{X}, \quad (4)$$

where all derivatives refer to the two-dimensional metric g_{ab} . Integrating over the angular coordinates, $\int d\Omega_2 = 4\pi$, yields

$$S_2 = \frac{1}{4G_4} \int d^2x \sqrt{-g} [XR + U(X)(\nabla X)^2 + 2V(X)], \quad (5)$$

with²

$$U(X) = \frac{1}{2X}, \quad V(X) = \frac{1}{2} - \frac{\Lambda}{2}X. \quad (6)$$

A. Weyl frame and SdS solution

In 2D it is possible to eliminate the dilaton kinetic term by performing a simple Weyl rescaling

$$\tilde{g}_{\mu\nu} = e^{Q(X)} g_{\mu\nu}, \quad Q'(X) = -U(X) = -\frac{1}{2X}, \quad (7)$$

¹ We closely follow the standard spherically reduced gravity (SRG) formalism [28–30].

² Note our V differs by a factor of 1/2 from some SRG conventions; this is absorbed into w and ξ below.

so that $Q(X) = -\frac{1}{2} \ln X$ and $e^{Q(X)} = X^{-1/2}$.

In this Weyl frame, the action becomes (up to boundary terms)

$$S_2 = \frac{1}{4G_4} \int d^2x \sqrt{-\tilde{g}} \left[X\tilde{R} + 2\tilde{V}(X) \right], \quad (8)$$

$$\tilde{V}(X) := e^{Q(X)}V(X) = X^{-1/2} \left(\frac{1}{2} - \frac{\Lambda}{2}X \right). \quad (9)$$

Introducing the auxiliary functions

$$w'(X) = \tilde{V}(X), \quad \xi(X) = e^{Q(X)}[w(X) - 2G_4M], \quad (10)$$

the general static solution reads

$$ds^2 = -\xi(r) dt^2 + \xi(r)^{-1} dr^2, \quad X = r^2. \quad (11)$$

Integration of Eq. 10 gives

$$\begin{aligned} w(X) &= \int^X \tilde{V}(y) dy = \int \left(\frac{1}{2r} - \frac{\Lambda}{2}r \right) 2r dr \\ &= r - \frac{\Lambda}{3}r^3 + \text{const.} \end{aligned} \quad (12)$$

Choosing the constant to vanish and using $e^Q = 1/r$, the metric function becomes

$$\xi(r) = \frac{1}{r}(w - 2G_4M) = 1 - \frac{2G_4M}{r} - \frac{\Lambda}{3}r^2, \quad (13)$$

which reproduces the familiar Schwarzschild–de Sitter blackening function.

III. SEMICLASSICAL TRACE–ANOMALY BACKREACTION

We work in the large- N semiclassical expansion of our spherically reduced gravity, in which the backreaction of N conformal matter fields is encoded by the two-dimensional Polyakov anomaly action. The full 2D effective action is

$$S_{\text{eff}} = S_2 + S_{\text{anom}}, \quad (14)$$

where S_2 is given by (5) with (6), and the Polyakov term captures the trace anomaly of N massless conformal fields,

$$S_{\text{anom}}[g] = -\frac{N}{96\pi} \int d^2x \sqrt{-g} R \square^{-1} R, \quad (15)$$

whose variation yields the anomalous trace $\langle T^{\mu}_{\mu} \rangle = (N/24\pi) R$. For practical computations we employ the equivalent local (auxiliary-field) form of S_{anom} given in Appendix A.

In conformal coordinates (u, v) with $ds^2 = -e^{2\rho(u,v)}du\,dv$, the renormalized expectation values of the stress tensor are

$$\begin{aligned}\langle T_{uu} \rangle &= -\frac{N}{12\pi}[(\partial_u \rho)^2 - \partial_u^2 \rho] + t_u(u), \\ \langle T_{vv} \rangle &= -\frac{N}{12\pi}[(\partial_v \rho)^2 - \partial_v^2 \rho] + t_v(v), \\ \langle T_{uv} \rangle &= -\frac{N}{12\pi} \partial_u \partial_v \rho,\end{aligned}\tag{16}$$

where t_u and t_v encode the quantum state (e.g. Unruh–dS thermal values). Regularity on the appropriate future Kruskal horizons fixes these constants: for the Unruh–de Sitter state, the future black-hole and cosmological horizons are regular, producing a steady flux between them.

Combining the classical and anomaly actions yields a closed, covariant system describing Hawking radiation, backreaction, and mass evolution in the Schwarzschild–de Sitter space-time. In what follows, we develop this framework to derive the conserved energy flux, the covariant mass–loss law, and the nonequilibrium thermodynamics of the system.

A. Conserved flux and mass–loss law

The steady Killing energy current admits a simple covariant formulation that directly yields the semiclassical mass–loss law. In the ingoing Eddington–Finkelstein (EF) gauge we have flux

$$\mathcal{J} := I(X) X'(r) T^r_v, \quad I(X) = e^{-Q(X)}, \quad Q'(X) = -U(X),\tag{17}$$

which is radially constant (and, to leading adiabatic order, slowly varying in v). For the Schwarzschild–de Sitter reduction $X = r^2$ and $I(X) = \sqrt{X} = r$, giving

$$\mathcal{J} = 2r^2 T^r_v.\tag{18}$$

Since $\chi = \partial_t = \partial_v$ in the stationary patch, the stress–tensor components coincide,

$$T^r_t = T^r_v = \frac{\mathcal{J}}{IX'} = \frac{\mathcal{J}}{2r^2},\tag{19}$$

so \mathcal{J} represents the single conserved Killing energy flux across the static patch.

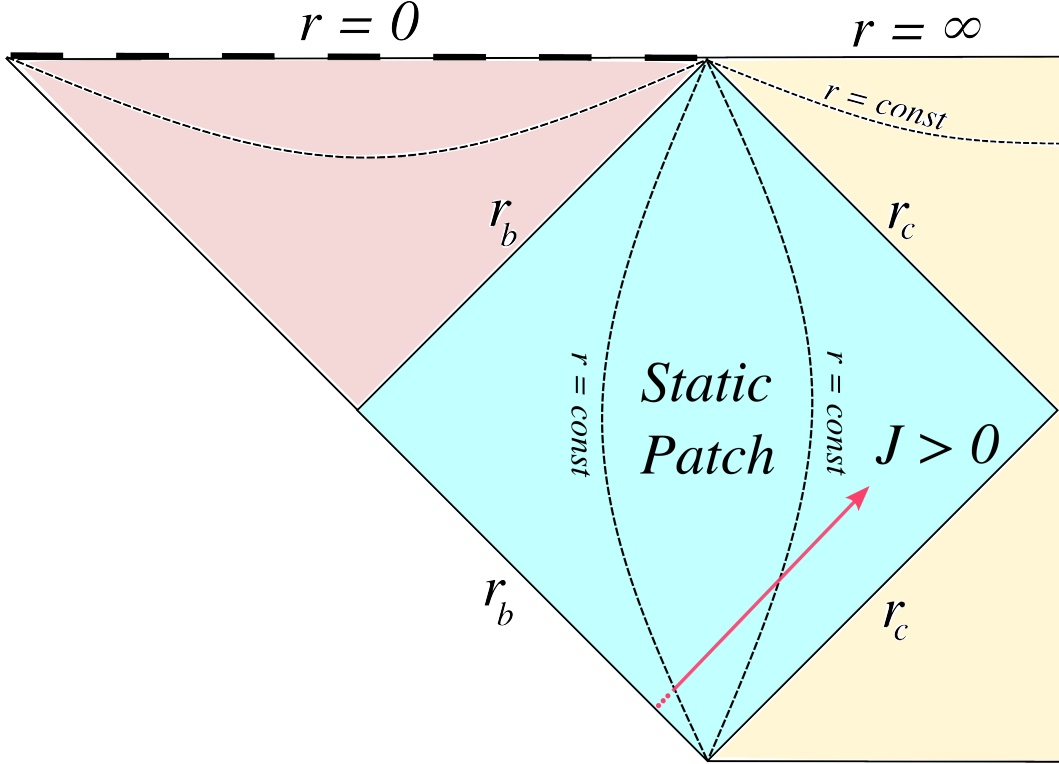


FIG. 1: Portion of the Penrose diagram for Schwarzschild–de Sitter emphasizing the static patch (blue). The patch is bounded by the black–hole (r_b) and cosmological (r_c) horizons. The black–hole singularity is at $r = 0$ (horizontal dashed line). Dashed curves represent surfaces of constant r . In the Unruh–de Sitter state, the anomaly–induced flux $\mathcal{J} > 0$ propagates outward from the hotter black–hole horizon to the cooler cosmological horizon, establishing a steady nonequilibrium state.

The EF Casimir (mass–function) balance law yields the covariant mass–loss relation

$$\dot{M} = -\mathcal{J}. \quad (20)$$

The detailed radial first integrals underlying this relation appear in Appendix A. Because the field equations do not admit a strictly static solution with $\mathcal{J} \neq 0$ (as proved in Appendix A), we work in the adiabatic steady–state regime, where M evolves slowly and the geometry remains quasi–static.

For the Schwarzschild–de Sitter metric the surface gravities at the horizons $r_h \in \{r_b, r_c\}$ are $\kappa_h = \frac{1}{2}|\xi'(r_h)|$. The geometry contains a finite static patch bounded by the black–hole and cosmological horizons (see Fig. 1), representing the causal domain of a stationary observer.

In the Unruh–de Sitter state, the anomaly–induced stress tensor admits a steady flux

$$\mathcal{J} = \frac{N}{48\pi} \Delta(M), \quad \Delta(M) \equiv \kappa_b^2 - \kappa_c^2, \quad (21)$$

directed outward for $\kappa_b > \kappa_c$. Identifying M with the total energy inside the static patch, the evolution follows

$$\dot{M} = -\frac{N}{48\pi} (\kappa_b^2 - \kappa_c^2), \quad (22)$$

so $\dot{M} < 0$.

Linearizing near a fixed point M_* gives

$$\frac{d}{dt} \delta M = -\frac{N}{48\pi} \Delta'(M_*) \delta M, \quad (23)$$

which is stable if $\Delta'(M_*) > 0$ and unstable if $\Delta'(M_*) < 0$. For neutral SdS, $\kappa_b = \kappa_c$ occurs only in the degenerate Nariai limit; thus no finite–temperature equilibrium exists within the static patch.

We assume the evaporation is slow ($|\dot{M}| \ll \kappa_b M$), so that at each instant the geometry remains approximately static (adiabatic approximation). This justifies treating the Hawking flux as spatially and temporally constant during the slow evaporation of M .³

The locally measured manifestation of this flux, together with the Tolman blueshift experienced by static observers, is analyzed in Sec. VII A.

B. Local temperatures and Tolman redshift

In conformal null coordinates, $ds^2 = -e^{2\rho} du dv$ (so that $e^{2\rho} = \xi$ in the static patch), the Polyakov stress tensor involves two state functions $t_u(u)$ and $t_v(v)$ which determine the flux components $\langle T_{uu} \rangle$ and $\langle T_{vv} \rangle$. Regularity on a future horizon with surface gravity κ_h fixes the corresponding function to $t_{u/v} = \kappa_h^2/4$, i.e. a thermal population at temperature

$$T_h = \frac{\kappa_h}{2\pi}. \quad (24)$$

Different quantum states correspond to different choices of (t_u, t_v) :

³ This approximation is well justified for large, slowly radiating black holes. As M approaches the Planck scale or the minimal mass allowed by the effective theory, the semiclassical and adiabatic descriptions necessarily break down and quantum–gravity effects are expected to dominate the final stage of evaporation.

- **Boulware–dS:** $t_u = t_v = 0$, static but singular on both horizons;
- **Hartle–Hawking–dS:** $t_u = t_v$ with $\kappa_b = \kappa_c$ (global thermal equilibrium, realized only at the Nariai point);
- **Unruh–dS:** $t_u = \kappa_b^2/4$, $t_v = \kappa_c^2/4$, regular on the future horizons and describing steady outward flux.

Static observers at $r \in (r_b, r_c)$ measure locally redshifted temperatures according to the Tolman–Ehrenfest relation $T_{\text{loc}}\sqrt{-g_{tt}} = \text{const}$ [31],

$$T_{h,\text{loc}}(r) = \frac{T_h}{\sqrt{\xi(r)}} = \frac{\kappa_h}{2\pi\sqrt{\xi(r)}}. \quad (25)$$

The ratio $T_{b,\text{loc}}/T_{c,\text{loc}} = \kappa_b/\kappa_c$ is position-independent, revealing the intrinsic nonequilibrium between the two horizons: only in the degenerate Nariai limit do the local temperatures coincide everywhere. This two-dimensional model exactly reproduces the four-dimensional temperature hierarchy and equilibrium condition of Schwarzschild–de Sitter spacetime, providing a faithful semiclassical reduction of the 4D thermodynamics. The resulting steady state carries a constant energy flux between the horizons, whose locally measured form is analyzed in Sec. VII A.

IV. EVAPORATION DYNAMICS AND MASS EVOLUTION

Using the flux Eq. 20, we now analyze the time evolution of the system under the anomaly–induced backreaction. The evolution of the mass parameter $M(t)$ follows from the interplay between the black-hole and cosmological surface gravities, which depend implicitly on M and Λ through the horizon equation $\xi(r_h; M, \Lambda) = 0$.

The static-patch metric with Eq. 13, admits two positive real roots $r_b < r_c$ when $0 < 9M^2\Lambda < 1$, defining the black-hole and cosmological horizons, bounding the causal diamond of a static observer. For fixed Λ , increasing M enlarges r_b and shrinks r_c , until they coincide at the Nariai limit $9M^2\Lambda = 1$.

The surface gravities at the horizons are

$$\kappa_b = \frac{M}{r_b^2} - \frac{\Lambda}{3}r_b, \quad \kappa_c = \frac{\Lambda}{3}r_c - \frac{M}{r_c^2}, \quad (26)$$

with $\kappa_b, \kappa_c > 0$ inside the static patch. Their difference determines the flux direction via $\Delta(M)$ (Eq. (21)).

As the black hole evaporates (M decreases), the black-hole horizon r_b contracts while the cosmological horizon r_c expands. Consequently κ_b rises rapidly, whereas κ_c increases from its small Nariai value toward the asymptotic limit $\sqrt{\Lambda/3}$. The growing temperature contrast Δ amplifies the Hawking flux, Eq. 21.

A. Flux, equilibrium and evolution timescales

The qualitative behavior of the system is governed by sign of $\Delta(M)$:

$$\begin{aligned}\Delta > 0 : \quad \dot{M} < 0 &\Rightarrow \text{evaporation (energy flow } b \rightarrow c\text{)}, \\ \Delta = 0 : \quad \dot{M} = 0 &\Rightarrow \text{thermal equilibrium}, \\ \Delta < 0 : \quad \dot{M} > 0 &\Rightarrow \text{anti-evaporation}.\end{aligned}$$

Fixed points M_* satisfy $\kappa_b(M_*) = \kappa_c(M_*)$, and linearization yields the stability condition $\Delta'(M_*) > 0$ (stable) or $\Delta'(M_*) < 0$ (unstable) (see Eq. (23)). Importantly, for uncharged SdS, $\kappa_b > \kappa_c$ throughout the static-patch domain, so $\Delta > 0$ and the mass decreases monotonically toward $M \rightarrow 0$. The sole equilibrium occurs at the Nariai boundary, where $\kappa_b = \kappa_c = 0$ and $\mathcal{J} = 0$.

The adiabatic evaporation timescale follows from Eq. (20):

$$\tau_{\text{evap}} \sim \frac{M}{|\dot{M}|} \simeq \frac{48\pi M}{N|\Delta(M)|}. \quad (27)$$

Evaporation is slow when the temperature contrast $|\Delta|^{1/2}$ is small and accelerates as $\kappa_b^2 \gg \kappa_c^2$. Near equilibrium, the relaxation is exponential with characteristic time

$$\tau_* \simeq \frac{48\pi}{N \Delta'(M_*)}.$$

As $M \rightarrow 0$, one finds $r_b \simeq 2M$, $\kappa_b \simeq (4M)^{-1}$, and $\kappa_c \simeq \sqrt{\Lambda/3}$, giving

$$\Delta \simeq \frac{1}{16M^2} - \frac{\Lambda}{3}, \quad \dot{M} \simeq -\frac{N}{768\pi} M^{-2}.$$

Hence $\tau_{\text{evap}} \sim 768\pi M^3/N$, reproducing the familiar M^3 scaling of four-dimensional Schwarzschild evaporation.

In principle, while three generic regimes exist:

1. **Monotonic evaporation:** $\Delta > 0$ everywhere $\Rightarrow M$ decreases to zero (neutral SdS).
2. **Stable equilibrium:** $\Delta(M)$ crosses zero with $\Delta'(M_*) > 0$.
3. **Unstable equilibrium:** $\Delta(M)$ crosses zero with $\Delta'(M_*) < 0$,

only the first regime occurs in the neutral black hole case; charged (Reissner-Nordström) or modified-gravity extensions may realize the others. We now analyze these equilibria in detail and identifies the Nariai configuration as the unique zero-flux limit.

V. QUASI-STATIONARY GEOMETRY FROM LOCALIZED POLYAKOV ACTION

In a strictly static metric ansatz, the off-diagonal (tr) equation enforces $T^r_t = 0$, so any exact static configuration must have vanishing flux ($J = 0$). The nonzero Unruh–de Sitter flux \mathcal{J} (the conserved energy current in the quasi–stationary state) therefore arises consistently only when time dependence is retained in Eddington–Finkelstein gauge, or within a quasi–stationary (adiabatic) approximation in which $M(v)$ evolves slowly compared to the local curvature scale. Throughout this section we use the term “steady state” in this adiabatic sense.

To describe this quasi-stationary configuration from first principles, we solve the field equations derived from the localized Polyakov action. The resulting geometry represents a fully backreacted, adiabatic steady state of the Unruh–de Sitter type, in which the flux \mathcal{J} is constant across the patch and mediates a net flow of energy from the black hole to the cosmological horizon. This solution demonstrates that the nonequilibrium evaporation dynamics of SdS in the Unruh–de Sitter state emerge self-consistently from the Einstein equations in two-dimensional dilaton gravity. In this analysis, all leading quantum effects are incorporated through the large- N , one-loop treatment of N conformal fields.

A. Localized action and semiclassical equations

The anomaly-induced Polyakov action can be written in local form by introducing an auxiliary field ψ :

$$S_P = -\frac{N}{96\pi} \int d^2x \sqrt{-g} \left[(\nabla\psi)^2 + 2\psi R \right], \quad (28)$$

whose equation of motion $\square\psi = R$ reproduces the trace anomaly. The full semiclassical action is

$$S = \frac{1}{4G_4} \int d^2x \sqrt{-g} [XR + 2\tilde{V}(X)] + S_{\text{P}}. \quad (29)$$

Variation yields the coupled dilaton and metric equations

$$R + 2\tilde{V}'(X) = 0, \quad \frac{1}{4G_4} (\nabla_\mu \nabla_\nu X - g_{\mu\nu} \square X - \tilde{V} g_{\mu\nu}) = T_{\mu\nu}^{(\psi)} + T_{\mu\nu}^{(\text{state})}. \quad (30)$$

with $T^{(\psi)\mu}_{\mu} = \frac{N}{24\pi} R$ and $T_{\mu}^{(\text{state})\mu} = 0$. Details of the first integrals and the static momentum constraint appear in Appendix A.

Near any simple horizon where $f(r) \simeq \kappa(r - r_h)$, regularity requires $C_\psi = 0$ in the local solution $f\psi' = -f' + C_\psi$, giving $\psi \simeq -\ln f + \text{const}$. In the strictly static ansatz this implies $T^r_t = 0$, while in the adiabatic Eddington–Finkelstein solution the physical flux is \mathcal{J} , related to the static-frame component Eq. 42.

B. Solution structure and horizon regularity

The equations derived from (29) form a closed ODE system for (f, X, ψ) that admits first integrals and a reduction to quadratures. Regularity of the renormalized stress tensor on the appropriate future Kruskal horizons (black hole and cosmological) imposes state-dependent boundary conditions consistent with the Unruh–de Sitter state. These conditions fix the state functions t_\pm , equivalently the conserved EF flux \mathcal{J} , yielding an adiabatic (quasi-stationary) solution that is exact at leading order in slow time.⁴ The instantaneous geometry is parametrized by the Casimir (mass) and flux, e.g. $(M, \Lambda, \mathcal{J})$, and continuously deforms the classical SdS spacetime while maintaining a radially conserved energy flux across the static patch. The first-integral structure and explicit quadratures are given in Appendix A, and the finiteness of the backreacted curvature invariants in the backreacted geometry is verified in Appendix D.

This adiabatic solution (closed form up to quadrature) provides a self-consistent, analytic framework for generalized-entropy and extremal-surface calculations: given $\langle T_{\mu\nu} \rangle$ and the Polyakov field, we compute $S_{\text{gen}} = S_{\text{Wald}}(X) + S_{\text{out}}(\mathcal{R} \cup I)$ in the Unruh–de Sitter state,

⁴ In conformal gauge, the renormalized stress tensor depends on two state functions t_\pm that encode the choice of quantum state (Boulware, Hartle–Hawking, or Unruh). In a stationary patch these are constants related by $\mathcal{J} = (N/48\pi)(t_+ - t_-)$ in our normalization, so specifying the flux \mathcal{J} is equivalent to fixing (t_+, t_-) .

locate QES via $\partial_{\pm}S_{\text{gen}} = 0$, and estimate Page-like behavior in a two-horizon setting at leading semiclassical order.

This same anomaly-induced backreaction that governs the semiclassical dynamics of the SdS patch also plays a decisive role in other multi-horizon systems. An analogous mechanism destabilizes the inner (Cauchy) horizons of charged and rotating black holes, where the trace anomaly is the minimal quantum enforcer of strong cosmic censorship [32] by converting inner horizons into null curvature singularities [33].

VI. EQUILIBRIUM CONFIGURATIONS AND STABILITY

Evaporation halts when the net Hawking flux between the black-hole and cosmological horizons vanishes. As derived in Eq. (21), this occurs when the two surface gravities coincide,

$$\kappa_b(M_*) = \kappa_c(M_*). \quad (31)$$

Such equal-temperature configurations define equilibrium points M_* for fixed Λ . In charged (Reissner–Nordström–de Sitter) spacetimes, these correspond to the well-known *lukewarm* black holes with $\kappa_b = \kappa_c \neq 0$. For the uncharged Schwarzschild–de Sitter case considered here, however, this equality is achieved only at the degenerate *Nariai* limit ($9M^2\Lambda = 1$), where the two horizons merge ($r_b = r_c$) and both surface gravities vanish. Hence, the Nariai geometry represents the unique zero-flux equilibrium configuration of the neutral SdS family.

To discover the sign of the flux away from equilibrium, we derive an explicit analytic expression for $\Delta = \kappa_b^2 - \kappa_c^2$. Eliminating M from the two horizon equations,

$$M = \frac{r_b}{2} \left(1 - \frac{\Lambda}{3} r_b^2\right) = \frac{r_c}{2} \left(1 - \frac{\Lambda}{3} r_c^2\right),$$

gives the fundamental horizon relation

$$1 = \frac{\Lambda}{3} \left(r_b^2 + r_b r_c + r_c^2\right). \quad (32)$$

Using this identity, the surface gravities satisfy

$$\kappa_b + \kappa_c = \frac{r_c - r_b}{2} \left(\Lambda + \frac{1}{r_b r_c}\right) > 0, \quad (33)$$

and, independently,

$$\kappa_b - \kappa_c = \frac{r_b + r_c}{2} \left(\frac{1}{r_b r_c} - \Lambda\right) > 0, \quad (34)$$

so that $\kappa_b > \kappa_c$ for all $0 < 9M^2\Lambda < 1$.

Hence,

$$\Delta(M) = (\kappa_b - \kappa_c)(\kappa_b + \kappa_c) > 0,$$

and (as one may have anticipated) the semiclassical flux

$$\mathcal{J} = \frac{N}{48\pi} \Delta(M)$$

is positive throughout the static patch, implying strictly monotonic mass loss ($\dot{M} < 0$) for all nonextremal configurations. Linearizing the evolution confirms that no finite-temperature equilibrium exists: the only zero-flux configuration is the degenerate Nariai state, which we discuss next.

A. The Nariai limit and zero-flux equilibrium

We have shown the SdS family admits a single equilibrium configuration where the black hole and cosmological horizons coincide. This extremal geometry, known as the *Nariai spacetime* [15, 34, 35], arises at the maximal mass

$$M_{\text{Nariai}} = \frac{1}{3\sqrt{\Lambda}}, \quad r_b = r_c = \frac{1}{\sqrt{\Lambda}}, \quad (35)$$

for which the surface gravities vanish $\kappa_b = \kappa_c = 0$. In this limit the SdS coordinates become degenerate, but after a suitable rescaling the metric factorizes as

$$ds^2 = \frac{1}{\Lambda} [-\sin^2\chi d\tau^2 + d\chi^2] + \frac{1}{\Lambda} d\Omega_2^2, \quad (36)$$

describing the direct product $dS_2 \times S^2$ with constant curvature $R = 2\Lambda$. The Nariai geometry therefore represents a zero-temperature equilibrium configuration of the SdS family in the standard static normalization, corresponding to the unique fixed point of the mass-loss equation. Perturbations away from this limit split the horizons and produce nearby SdS solutions with $\kappa_b > \kappa_c$, initiating nonequilibrium energy flow from the black hole to the cosmological horizon.

In our two-dimensional dilaton gravity description, the Nariai state is realized when the effective potential satisfies

$$\tilde{V}(X_N) = 0, \quad X_N = \frac{1}{\Lambda}, \quad (37)$$

so that $w'(X_N) = 0$ and the Killing function $\xi(X)$ develops a double root. The anomaly-induced flux, Eq. 21, then vanishes $\mathcal{J} = 0$, confirming that the Nariai limit marks the sole equilibrium point in the (M, Λ) phase diagram.

For the observed cosmological constant, $\Lambda \simeq 10^{-52} \text{ m}^{-2}$, the Nariai horizon radius is $r_{\text{Nariai}} = 1/\sqrt{\Lambda} \sim 10^{26} \text{ m}$, and the corresponding mass is $M_{\text{Nariai}} \simeq c^2/(3G_4\sqrt{\Lambda}) \approx 2.3 \times 10^{22} M_\odot$. This mass is cosmologically large, comparable to the total mass contained within the observable universe, and represents the unstable upper mass bound for a black hole in the Schwarzschild–de Sitter family. All known black holes (from stellar to supermassive, $\sim 10\text{--}10^{10} M_\odot$) lie deep in the $M \ll M_{\text{Nariai}}$ regime. As the semiclassical flux law (Eq. 22) is shown in Appendix B to remain evaporative ($\dot{M} < 0$) for this entire physical range, the Nariai configuration is never approached dynamically. Consequently, the only physically attainable endpoint of SdS black-hole evaporation in our de Sitter background is the empty de Sitter state.

We now map these regimes across (M, Λ) parameter space and identify the Nariai line $9M^2\Lambda = 1$ as the boundary separating the evaporation domain from the degenerate equilibrium configuration.

B. Phase diagram

The equilibrium set $\Delta(M, \Lambda) = 0$ reduces, for neutral SdS, to the Nariai curve $9M^2\Lambda = 1$, which forms the boundary of the physical static-patch domain. Within the domain $0 < 9M^2\Lambda < 1$ one has $\Delta > 0$, so the flux direction does not change sign.

The sign of $\Delta'(M)$ above and below this line determines whether the evolution is attractive or repulsive, yielding a semiclassical *phase diagram* of SdS evaporation (see Fig. 2). The values of Λ shown are far larger than the observed cosmological constant but the analysis cleanly isolates the qualitative structure of the evaporation dynamics. No nondegenerate equilibrium configuration exists within the static patch: the anomaly-induced flux drives the black hole mass monotonically toward $M \rightarrow 0$ (empty de Sitter), with the Nariai boundary marking the unique zero-flux limit that separates evaporating from unphysical regions of parameter space.

Having established the global structure of evaporation and the location of equilibrium boundaries in (M, Λ) space, we now turn to the thermodynamics experienced by local static

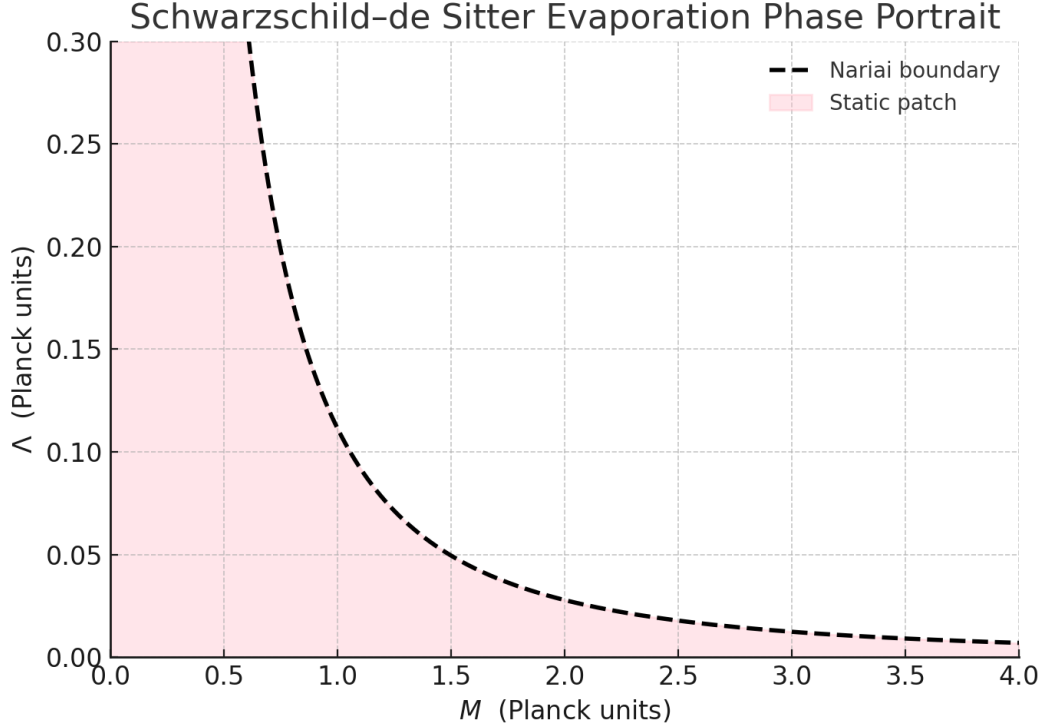


FIG. 2: Evaporation phase diagram for Schwarzschild-de Sitter black holes. Each point (M, Λ) with $0 < 9M^2\Lambda < 1$ represents a physical static patch. Throughout this domain $\Delta > 0$, corresponding to a steady energy flux from the black-hole to the cosmological horizon ($\dot{M} = -\mathcal{J} < 0$). The dashed curve marks the Nariai boundary $9M^2\Lambda = 1$, where the two horizons coincide and attain equal surface gravities (see Sec. VI A). All quantities are in Planck units ($G_4 = \hbar = c = 1$).

observers within the de Sitter static patch.

VII. OBSERVER-DEPENDENT THERMODYNAMICS

In the static patch of SdS, stationary observers experience distinct local thermodynamic conditions depending on their position between the black hole and cosmological horizons. The region $r_b < r < r_c$ admits the timelike Killing field $\chi^\mu = \partial_t$ with norm $\chi^2 = g_{\mu\nu}\chi^\mu\chi^\nu = -\xi(r)$. Static observers follow orbits of χ^μ with four-velocity

$$u^\mu = \frac{\chi^\mu}{\sqrt{-\chi^2}} = \frac{1}{\sqrt{\xi(r)}}(1, 0), \quad e_{(\hat{r})}^\mu = \sqrt{\xi(r)}(0, 1), \quad (38)$$

defining the orthonormal frame $\{u^\mu, e_{(\hat{r})}^\mu\}$.

A. Local temperatures and steady flux

Building on the Tolman relation introduced in Sec. III B, we now evaluate the locally measured energy flux and density experienced by static observers in the Schwarzschild–de Sitter static patch.

Each Killing horizon $r_h \in \{r_b, r_c\}$ possesses surface gravity $\kappa_h = \frac{1}{2}|\xi'(r_h)|$ and Hawking temperature $T_h = \kappa_h/(2\pi)$. A static observer at radius r measures the redshifted temperature

$$T_{h,\text{loc}}(r) = \frac{T_h}{\sqrt{\xi(r)}} = \frac{\kappa_h}{2\pi\sqrt{\xi(r)}}, \quad (39)$$

so that $T_{b,\text{loc}}/T_{c,\text{loc}} = \kappa_b/\kappa_c$. The patch is therefore intrinsically out of equilibrium whenever $\kappa_b \neq \kappa_c$; only in the Nariai (lukewarm) limit do the local temperatures coincide.

To quantify this nonequilibrium steady state, let $\langle T_{\mu\nu} \rangle$ denote the renormalized stress tensor in the chosen quantum state. For static observers with four-velocity $u^\mu = (1/\sqrt{\xi}, 0)$ and orthonormal radial vector $e_{(\hat{r})}^\mu = (0, \sqrt{\xi})$, the locally measured energy density and radial flux are

$$\begin{aligned} \rho(r) &= \langle T_{\mu\nu} \rangle u^\mu u^\nu, \\ \mathcal{F}_{\text{loc}}(r) &= -\langle T_{\mu\nu} \rangle u^\mu e_{(\hat{r})}^\nu = -\frac{T^r_t}{\xi(r)}. \end{aligned} \quad (40)$$

Stationarity implies $\nabla_\mu T^\mu_t = 0$, so the mixed component T^r_t (and therefore the Killing energy flux \mathcal{J}) is constant throughout the patch:

$$T^r_t = \frac{\mathcal{J}}{2r^2} = \text{const.} \quad (41)$$

Projecting onto the local frame gives

$$\mathcal{F}_{\text{loc}}(r) = -\frac{\mathcal{J}}{2r^2\xi(r)}, \quad (42)$$

which blueshifts as $1/\xi(r)$ toward either horizon. Hence the SdS static region acts as a finite thermal cavity bounded by two horizons at unequal Tolman temperatures, linked by a conserved heat current \mathcal{J} that vanishes only in the Nariai equilibrium configuration.

Physically, $\mathcal{J} > 0$ corresponds to an outward flux of Killing energy from the hotter black-hole horizon to the cooler cosmological horizon. The same flux governs the global mass-loss law $\dot{M} = -\mathcal{J}$ derived in Sec. III A, ensuring that the locally observed nonequilibrium and the global evaporation dynamics are two aspects of the same conserved-energy flow.

B. Near-horizon behavior and regularity

Near each Killing horizon, it is convenient to express the metric in conformal gauge,

$$ds^2 = -e^{2\rho} du dv, \quad e^{2\rho} = \xi(r).$$

The anomaly-induced stress tensor then takes the form (16), where t_u and t_v are the state-dependent constants specifying the ingoing and outgoing flux components in a stationary patch.

Regularity on a given future horizon fixes the corresponding constant to its thermal value at $T_h = \kappa_h/(2\pi)$: t_u at the future black-hole horizon and t_v at the future cosmological horizon. The *Unruh-de Sitter* state enforces regularity on both future horizons while remaining singular on the past ones, yielding the steady flux (21). In contrast, the *Boulware-de Sitter* state has $t_u = t_v = 0$ and is singular on all horizons, while the *Hartle-Hawking-de Sitter* state occurs only at the Nariai limit [36].

C. Detector response

A standard static Unruh–DeWitt detector following the worldline $x^\mu(\tau)$ with four-velocity u^μ interacts locally with the quantum field and can become excited by absorbing a quantum of energy Ω . The quantity $\mathcal{P}(\Omega; r)$ denotes the corresponding transition probability, and $\dot{\mathcal{P}}(\Omega; r)$ its excitation rate per unit proper time. At leading order in perturbation theory this rate is given by

$$\dot{\mathcal{P}}(\Omega; r) = \int_{-\infty}^{+\infty} d\tau e^{-i\Omega\tau} G^+(x(\tau), x(0)), \quad (43)$$

where G^+ is the Wightman function in the chosen quantum state. In the stationary patch (Unruh–de Sitter state), the response decomposes into thermal contributions from each horizon, each redshifted by the Tolman factor $1/\sqrt{\xi(r)}$ as in (25). The resulting detailed-balance condition encodes the conserved flux \mathcal{J} : the net excitation probability is nonzero whenever the two horizon temperatures differ and vanishes at thermal equilibrium (the Nariai boundary; see Sec. VI A).⁵

⁵ Static detectors have infinite proper acceleration near the horizons, so their locally measured flux diverges as $1/\sqrt{\xi}$. This is a coordinate effect; the renormalized stress tensor remains finite in freely falling frames.

VIII. ENTROPY FLOW AND THE GENERALIZED SECOND LAW

The coexistence of two horizons in SdS raises subtle questions about how gravitational entropy evolves during evaporation. Here we show that the anomaly-induced flux \mathcal{J} automatically satisfies the generalized second law (GSL) throughout the evaporation process, as expected. In a quasistationary process, the Hawking radiation within the static patch forms a steady flow rather than an accumulating bath; its entropy therefore remains constant in time, $\dot{S}_{\text{out}} = 0$. The only entropy changes arise from the horizons themselves, so that the generalized entropy evolves as

$$\dot{S}_{\text{gen}} = \dot{S}_b + \dot{S}_c. \quad (44)$$

A. Entropy balance and first-law structure

Let $S_b = \pi X_b/G_4$ and $S_c = \pi X_c/G_4$ denote the Wald entropies of the black-hole and cosmological horizons ($X = r^2$). At fixed Λ , the static SdS family obeys the parametric identity

$$\delta M = T_b \delta S_b - T_c \delta S_c, \quad (45)$$

where the minus sign reflects the opposite Killing orientation of the cosmological horizon. This “first law” describes variations among nearby static configurations and should not be interpreted as a dynamical evolution equation. The time-dependent semiclassical evolution is governed instead by the conserved energy flux.

1. Flux balance and horizon Clausius relations

Energy conservation implies a single radially conserved flux of Killing energy across the patch. Defining $\mathcal{J} > 0$ as the outward (increasing- r) flux measured by static observers, each horizon obeys its own local Clausius relation,

$$T_b \dot{S}_b = -\mathcal{J}, \quad T_c \dot{S}_c = +\mathcal{J}, \quad (46)$$

expressing that the black hole loses heat while the cosmological horizon gains the same amount. The net Killing-energy balance of the entire patch is

$$\dot{M} = -\mathcal{J}, \quad (47)$$

so that each relation in (46) may equivalently be written as

$$\dot{M} = T_b \dot{S}_b = -T_c \dot{S}_c.$$

Equation (45) therefore serves as a geometric identity among neighboring static configurations, whereas (46)–(47) govern the true time-dependent evolution driven by the anomaly-induced flux.

2. Generalized second law

Combining (46) gives the total gravitational entropy production rate,

$$\dot{S}_{\text{gen}} = \dot{S}_b + \dot{S}_c = \mathcal{J} \left(\frac{1}{T_c} - \frac{1}{T_b} \right) > 0 \quad (\kappa_b > \kappa_c), \quad (48)$$

showing that after the decrease in black-hole entropy, the cosmological horizon's increase more than compensates, ensuring the monotonic growth of the total generalized entropy. When $T_b = T_c$ (the Nariai limit), $\mathcal{J} = 0$ and $\dot{S}_{\text{gen}} = 0$, indicating exact thermal equilibrium.

For conformal matter, the anomaly-induced flux $\mathcal{J} = (\pi N/12)(T_b^2 - T_c^2)$ reproduces the steady-state relation of a 1+1-dimensional CFT, and the entropy production rate becomes

$$\dot{S}_{\text{gen}} = \frac{\pi N}{12} \frac{(T_b - T_c)^2 (T_b + T_c)}{T_b T_c} \geq 0, \quad (49)$$

with equality only in the Nariai configuration. Thus, throughout the physical static-patch domain $0 < 9M^2\Lambda < 1$, the Unruh–de Sitter state satisfies $\mathcal{J} > 0$ and $\dot{S}_{\text{gen}} > 0$, while in the degenerate Nariai limit (where the horizons coincide and the temperature contrast vanishes) the flux and entropy production both go to zero. These relations hold on the two-horizon patch domain. In the formal endpoint $M \rightarrow 0$, the black-hole horizon disappears and T_b is no longer defined; the steady two-horizon flux formula is therefore inapplicable, and the state smoothly reduces to the de Sitter vacuum with no inter-horizon flux. The 2D anomaly framework provides a fully analytic and self-consistent realization of the generalized second law for spacetimes with multiple horizons.

IX. QUANTUM EXTREMAL SURFACES AND ENTANGLEMENT ISLANDS

The SdS solution constructed above naturally lends itself to the study of quantum extremal surfaces (QES) and entanglement islands in a cosmological setting. Recent developments in semiclassical gravity have shown that these quantum surfaces (stationary points

of the generalized entropy functional) play a central role in the unitary description of black hole evaporation [37–39]. While most existing analyses are carried out in asymptotically flat or AdS spacetimes, the Schwarzschild–de Sitter geometry provides a conceptually distinct testing ground with two horizons and a finite static patch.

A. Generalized entropy and QES conditions

In our 2D effective theory, the generalized entropy of a region \mathcal{R} with boundary $\partial\mathcal{R}$ is

$$S_{\text{gen}}[\partial\mathcal{R}] = \frac{X(\partial\mathcal{R})}{4G_2} + S_{\text{out}}[\mathcal{R}], \quad (50)$$

where the first term represents the Bekenstein–Hawking (dilaton) entropy of the boundary surface, and S_{out} is the von Neumann entropy of quantum fields in \mathcal{R} . The two-dimensional Newton constant G_2 is defined so that $S_{\text{BH}} = X/4G_2$ reproduces the usual four-dimensional area law; for spherical reduction one has $G_2 = G_4/(4\pi)$, ensuring $S_{\text{BH}} = \pi X/G_4 = X/(4G_2)$.⁶

A quantum extremal surface (QES) is a stationary point of the generalized entropy,

$$\partial_{\pm}S_{\text{gen}} = \frac{1}{4G_2} \partial_{\pm}X + \partial_{\pm}S_{\text{out}} = 0, \quad (51)$$

where ∂_{\pm} denote derivatives along the outgoing and ingoing null directions k_{\pm}^{μ} of the metric $ds^2 = -e^{2\rho(u,v)}du\,dv$ (with $\partial_{\pm} \equiv k_{\pm}^{\mu}\nabla_{\mu}$). These equations express the vanishing of the “quantum expansions” of S_{gen} and reduce to the usual extremality of the area term when quantum effects are neglected.

For conformal matter, S_{out} can be computed directly from the conformal factor and the state-dependent functions that determine $\langle T_{\mu\nu} \rangle$. In a smooth metric $ds^2 = -e^{2\rho}du\,dv$, the entropy of an interval with endpoints $p_i = (u_i, v_i)$ is

$$S_{\text{out}}(p_1, p_2) = \frac{c}{6} \left[\rho(p_1) + \rho(p_2) + \ln \frac{|u_1 - u_2| |v_1 - v_2|}{\epsilon_1 \epsilon_2} \right] + \delta_{\text{state}}, \quad (52)$$

where $c = N$ is the central charge, ϵ_i are short-distance cutoffs, and δ_{state} encodes the conformal transformation to coordinates regular on the relevant future horizons. In our

⁶ In four dimensions the Bekenstein–Hawking entropy is $S = A/(4G_4)$, with $A = 4\pi r_B^2$. Under spherical reduction the dilaton is defined by $X = r^2$, so that $A = 4\pi X$ and the reduced coupling $G_2 = G_4/(4\pi)$ yields $S_{\text{BH}} = \pi X/G_4 = X/(4G_2)$. Thus X plays the role of the horizon area in the two-dimensional theory.

setup, the state is characterized by the constants (t_u, t_v) that fix the Unruh–de Sitter flux and determine both $\langle T_{\mu\nu} \rangle$ and the additive terms in S_{out} .⁷

B. Islands in the static patch

In the SdS static patch, a natural entanglement region \mathcal{R} is the domain accessible to a static observer at fixed $r < r_c$, bounded by the cosmological horizon. Radiation emitted from the black-hole horizon propagates outward and becomes causally inaccessible to the static observer beyond r_c . Our explicit anomaly-induced backreaction and steady flux framework provides a background to analyze the information flow.

As the coarse-grained entropy of the outgoing radiation increases, a stationary point of the generalized entropy S_{gen} can develop just inside the black-hole horizon r_b , marking the formation of an island whose interior lies beyond the horizon but whose entanglement wedge is contained within the static patch accessible to the observer.⁸

At this point the dominant saddle in the path integral shifts from the no-island configuration to one that includes the island. This transition represents the de Sitter analogue of a Page transition. Because both the anomaly-induced stress tensor and the Polyakov field are known analytically in our model, the framework is ideally suited to a fully analytic treatment of QES and the Page curve in multi-horizon spacetimes.

1. Entanglement structure

In the de Sitter static patch, the radiation field is not entangled solely with the black-hole interior (as in asymptotically flat evaporation) but also with degrees of freedom associated with the cosmological horizon. The global state of the full SdS spacetime is pure, yet a static observer has access only to the inter-horizon region. The relevant entanglement structure is therefore tripartite, $(\mathcal{H}_{\text{BH}} \otimes \mathcal{H}_{\text{rad}} \otimes \mathcal{H}_{\text{ds}})$, where each \mathcal{H} denotes the Hilbert space of the corresponding subsystem and the fine-grained entropy accessible within the static patch is

⁷ In the stationary Unruh–de Sitter state, the local energy and entropy densities are time-independent, but the coarse-grained entropy carried by the steady radiation flow increases linearly with time at the rate $\dot{S}_{\text{prod}} = \mathcal{J} \left(\frac{1}{T_c} - \frac{1}{T_b} \right)$. In the time-dependent island analysis, S_{rad} denotes this coarse-grained von Neumann entropy of the emitted radiation.

⁸ In the two-dimensional reduction, the quantum extremal surface is a single spatial point r_I (or a pair of points on opposite sides of the Penrose diagram), so the “island” corresponds to the interval between this point and the observer’s region \mathcal{R} .

bounded by the black-hole entropy, $S_{\text{rad}}(t) \leq S_b(t)$, up to correlations with the cosmological horizon. The Page transition corresponds to the point at which an island forms near the black-hole horizon, incorporating its interior into the entanglement wedge of the radiation and restoring unitary information balance within the patch.

Our Page-curve analysis employs a two-dimensional dilaton reduction in which gravity has no local propagating degrees of freedom; the only fields with long-range tails are the conformal matter sectors entering the Polyakov action. In this setting, the Gauss-law constraints and gravitational dressings that obstruct Hilbert-space factorization in theories with dynamical (massless) gravitons are absent. Although diffeomorphism constraints remain, there is no soft-graviton sector, so the standard island prescription can be applied without additional edge-mode bookkeeping. Consequently, our results should be read as evidence *within this controlled model* that, when long-range dressings are under control, the island mechanism operates consistently in the de Sitter static patch.

Recent work has emphasized conceptual issues for massless gravity and gauge theories, where factorization fails due to soft modes and global constraints (see, e.g., [40–44]). Our 2D dilaton model sidesteps these issues by construction, providing a semiclassical test-bed in which the island mechanism is unambiguous. Extending the analysis to retain four-dimensional soft-graviton sectors (including edge modes at the cosmological horizon and their charges) is an interesting open problem that would more directly address concerns specific to massless gravity.⁹

2. *Cosmological counterpart*

By symmetry, a complementary quantum extremal surface (QES) can lie just inside the cosmological horizon r_c , corresponding to an island for observers whose algebra is anchored outside the static patch, in the neighboring de Sitter region. In the *Unruh–de Sitter* state considered here, the steady flux is directed outward from the black-hole horizon toward the cosmological horizon. For observers within the static patch, this makes the inner island near r_b the dynamically relevant saddle, while a cosmological-side island would instead be relevant to observers anchored beyond r_c . In time-reversed Unruh states the roles of the

⁹ Some braneworld constructions realize islands alongside an effectively massive graviton on the brane, but islands do not *require* massive gravity. In the present 2D dilaton model, there is no propagating graviton at all, and the island construction remains consistent.

horizons interchange.

In true equal-temperature (*lukewarm*) equilibrium there is no net flux: symmetric island saddles may then exist, for instance in charged Reissner–Nordström–de Sitter families. For the neutral Schwarzschild–de Sitter geometry, however, equality of the horizon temperatures occurs only in the degenerate Nariai limit. In all cases, candidate island endpoints satisfy the extremality conditions $\partial_{\pm}S_{\text{gen}} = 0$; which saddle dominates and the onset of the island phase (Page time) depend on the choice of quantum state and the flux orientation, and will be quantified below.

C. A thermo-controlled Page-curve estimate

We refer to this construction as *thermo-controlled* because the growth and turnover of the radiation entropy are determined entirely by macroscopic thermodynamic quantities: the horizon temperatures and steady flux, rather than by microscopic unitary dynamics.

As we have determined, in the Unruh–de Sitter state with $\kappa_b > \kappa_c$, the static patch supports a steady outward Killing flux

$$\mathcal{J} = \frac{N}{48\pi}(\kappa_b^2 - \kappa_c^2) = \frac{N\pi}{12}(T_b^2 - T_c^2), \quad T_h = \frac{\kappa_h}{2\pi}. \quad (53)$$

The corresponding irreversible (local) entropy production rate (Sec. VIII) is

$$\dot{S}_{\text{prod}} = \mathcal{J} \left(\frac{1}{T_c} - \frac{1}{T_b} \right) > 0 \quad (\kappa_b > \kappa_c \text{ or } T_b > T_c), \quad (54)$$

representing a steady flow of heat and entropy from the black-hole to the cosmological horizon.

To leading adiabatic order, the same rate governs the growth of the coarse-grained radiation entropy observed within the static patch,

$$\dot{S}_{\text{rad}}(t) \simeq \mathcal{J} \left(\frac{1}{T_c} - \frac{1}{T_b} \right), \quad S_{\text{rad}}(t) \simeq \mathcal{J} \left(\frac{1}{T_c} - \frac{1}{T_b} \right) t, \quad (55)$$

yielding a linear pre-Page growth whose slope is set entirely by the two-horizon thermodynamics. (Greybody effects or nonconformal corrections modify only the numerical coefficients.)

1. Refined Page condition

The Page time t_{Page} is defined as the moment when the generalized entropies of the two competing saddles become equal,

$$S_{\text{gen}}^{(\text{no-island})}(t_{\text{Page}}) = S_{\text{gen}}^{(\text{island})}(t_{\text{Page}}).$$

At the semiclassical level this equality is well approximated by two standard assumptions: (i) the no-island saddle is dominated by the coarse-grained radiation entropy S_{rad} , and (ii) the island saddle is dominated by the black hole's Bekenstein–Hawking entropy S_b . Under these approximations, the Page condition simplifies to

$$S_{\text{rad}}(t_{\text{Page}}) \simeq S_b(t_{\text{Page}}). \quad (56)$$

Using $\dot{M} = -\mathcal{J}(M)$ and $\dot{S}_{\text{rad}} = \mathcal{J}(M)\left(\frac{1}{T_c(M)} - \frac{1}{T_b(M)}\right)$, one can eliminate $\mathcal{J}(M)$ to obtain

$$\frac{dS_{\text{rad}}}{dM} = -\left(\frac{1}{T_c(M)} - \frac{1}{T_b(M)}\right), \quad (57)$$

which integrates to

$$S_{\text{rad}}(M) = \int_M^{M_0} \left(\frac{1}{T_c(m)} - \frac{1}{T_b(m)}\right) dm. \quad (58)$$

The Page condition (56) therefore becomes

$$\int_{M_{\text{Page}}}^{M_0} \left(\frac{1}{T_c} - \frac{1}{T_b}\right) dm = S_b(M_{\text{Page}}), \quad (59)$$

with $S_b(M) = \pi r_b(M)^2/G_4$ and $r_b(M)$ defined by $\xi(r_b; M, \Lambda) = 0$.

The corresponding Page time follows from the adiabatic relation

$$t_{\text{Page}} = \int_{M_{\text{Page}}}^{M_0} \frac{dm}{\mathcal{J}(m)} = \frac{48\pi}{N} \int_{M_{\text{Page}}}^{M_0} \frac{dm}{\kappa_b^2(m) - \kappa_c^2(m)}. \quad (60)$$

Because T_b increases as the black hole shrinks, S_{rad} grows faster than the frozen-temperature estimate predicts, so $S_b(t_{\text{Page}}) < S_b(0)$ and the true Page time occurs earlier than the naive constant-slope approximation.

Figure 3 contrasts the coarse-grained radiation entropy, obtained by integrating the adiabatic relation

$$\dot{S}_{\text{rad}}(t) = \mathcal{J}(M(t)) \left(\frac{1}{T_c(M(t))} - \frac{1}{T_b(M(t))}\right), \quad \dot{M}(t) = -\mathcal{J}(M(t)),$$

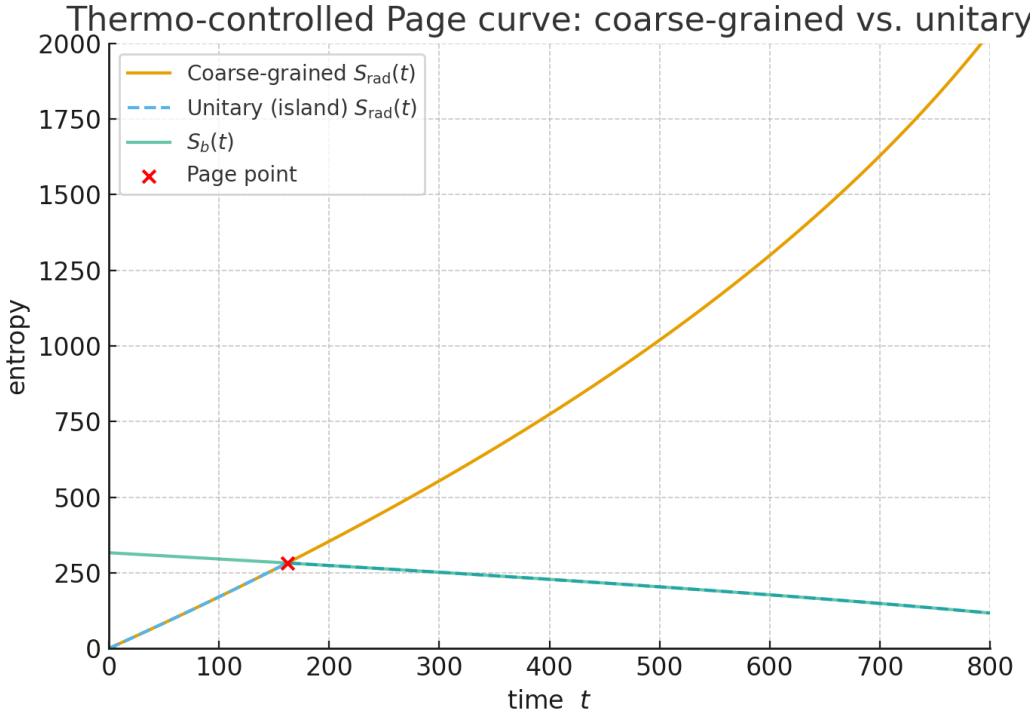


FIG. 3: Thermo-controlled Page curve for Schwarzschild–de Sitter. The solid (yellow) curve shows the coarse-grained radiation entropy $S_{\text{rad}}(t)$ obtained from the steady-state flux [Eqs. (53), (55)]. The dashed (blue) curve depicts the unitary (island) entropy $S_{\text{rad}}^{(\text{unitary})}(t) = \min\{S_{\text{rad}}(t), S_b(t)\}$, which turns over at the Page point (red marker) where the island saddle dominates [Eqs. (56)–(60)]. The (green) curve is the black-hole entropy $S_b(t)$. The cosmological horizon enters through T_c and the anomaly-induced flux; no additional fit parameters are introduced. (Parameters shown are representative; the qualitative behavior is robust for all $0 < 9M^2\Lambda < 1$.)

with $\mathcal{J}(M)$ given by Eq. (53), against the unitary (island) result

$$S_{\text{rad}}^{(\text{unitary})}(t) = \min\{S_{\text{rad}}(t), S_b(t)\}.$$

The turnover at t_{Page} (red marker) realizes the saddle switch implied by Eqs. (56)–(60), restoring unitarity in the late-time regime where the island contribution dominates. In this construction, the cosmological horizon is accounted for through T_c and the anomaly-induced flux \mathcal{J} , so no additional radiation reservoir needs to be introduced. The qualitative features—linear pre-Page growth determined by the two-horizon temperature contrast, followed by an island-controlled decrease tracking $S_b(t)$ —are insensitive to greybody effects

and persist throughout the neutral Schwarzschild–de Sitter domain $0 < 9M^2\Lambda < 1$.¹⁰

Since both $\mathcal{J}(m)$ and $(1/T_c - 1/T_b)(m)$ increase as M decreases, freezing them at their initial values underestimates the slope of $S_{\text{rad}}(t)$. Consequently,

$$t_{\text{Page}} \leq \frac{S_b(0)}{\mathcal{J}_0\left(\frac{1}{T_{c0}} - \frac{1}{T_{b0}}\right)}, \quad (61)$$

which serves as a conservative upper bound rather than a precise prediction.

A few comments are in order: (i) The slope in (55) matches the 1+1-dimensional CFT nonequilibrium steady-state relation $\mathcal{J} = \frac{\pi c}{12}(T_b^2 - T_c^2)$ with central charge $c = N$, now obtained directly from the Polyakov stress tensor in a curved two-horizon geometry. This provides the first fully analytic, anomaly-induced demonstration that the generalized second law is satisfied in Schwarzschild–de Sitter evaporation. (ii) Equations (59)–(60) show that increasing N or the temperature contrast $(T_b - T_c)$ shortens t_{Page} , while larger initial entropy $S_b(0)$ delays it. (iii) A microscopic QES derivation extremizes $S_{\text{gen}}[\partial\mathcal{I}] = \frac{X(\partial\mathcal{I})}{4G_2} + S_{\text{out}}(\mathcal{R} \cup \mathcal{I})$; in the adiabatic limit, the island endpoint lies exponentially close to the black-hole horizon, reproducing the same turnover at t_{Page} .

The inclusion of quantum extremal surfaces restores a Page-like entropy evolution within the semiclassical framework, ensuring that the generalized entropy of the radiation obeys unitarity bounds. However, this construction remains an *effective* resolution of the information paradox: the island prescription reproduces the fine-grained Page curve using semiclassical gravity supplemented by the Polyakov anomaly and replica-wormhole saddles, but it does not yet reveal the microscopic mechanism by which information escapes in Hawking quanta. In this sense, islands verify the *consistency* of semiclassical gravity with unitarity, rather than proving unitarity from first principles.

Although a full evaluation of S_{out} and the exact island geometry is beyond the present scope, our solvable SdS model provides a controlled solvable setting for exploring Page-like behavior in cosmological spacetimes, extending the modern island paradigm to multi-horizon backgrounds [45].

¹⁰ The Page point in Fig. 3 does not occur when the black hole has lost half of its initial entropy. In Schwarzschild–de Sitter spacetime, the presence of the cosmological horizon and the steady flux modify the entropy balance, so the condition $S_{\text{rad}} \simeq S_b$ replaces the heuristic $S_b \simeq \frac{1}{2}S_b(0)$ of single-horizon models.

X. CONCLUSIONS

Here we summarize our main conclusions and discuss possible future research directions. While our results accord with general expectations from black-hole thermodynamics, the framework developed here provides a fully analytic, backreacted realization of Schwarzschild–de Sitter evaporation, demonstrating explicitly that the anomaly-induced flux, horizon Clausius relations, and generalized second law coexist consistently within a single solvable model.

A. Main conclusions

- The conserved Hawking flux \mathcal{J} (Sec. III) drives the semiclassical evolution of the mass according to Eq. (20), representing steady energy transport from the black-hole to the cosmological horizon. Since $\Delta > 0$ for all neutral SdS configurations, the flux is always outward and the black-hole mass decreases monotonically.
- The system generically occupies a steady nonequilibrium state with $\kappa_b > \kappa_c$, in which radiation flows from the hotter to the cooler horizon. True thermal equilibrium occurs only when $\kappa_b = \kappa_c$, i.e. at the Nariai boundary where both surface gravities vanish and $\mathcal{J} = 0$.
- The (M, Λ) phase diagram shows that the entire static-patch region $0 < 9M^2\Lambda < 1$ lies in the evaporation regime. The Nariai configuration marks the unique zero-flux fixed point where the horizons coincide.
- Locally measured quantities, such as temperature, flux, and energy density, obey Tolman redshift and behave as expected for a finite thermal cavity bounded by walls at unequal temperatures.
- The GSL holds throughout the semiclassical evolution: although S_b decreases, S_c increases more rapidly, ensuring that the total generalized entropy $S_{\text{gen}} = S_b + S_c$ grows monotonically.
- Extending beyond thermodynamics, the same framework reproduces Page-like information recovery: the radiation entropy grows linearly at a rate fixed by the tem-

perature contrast and steady flux, and saturates at the Page time when the island contribution is consistent with unitarity. This unifies semiclassical thermodynamics and information flow in a single analytic model.

These results highlight the effectiveness of the two-dimensional anomaly-induced framework for capturing both the thermodynamic and informational aspects of black holes with multiple horizons. Within the semiclassical approximation the mass decreases monotonically and the black hole evaporates completely, leaving an empty de Sitter static patch. Once M becomes comparable to the Planck mass, however, the effective two-dimensional description ceases to be reliable, and phenomena such as a final burst of Hawking radiation or a short-lived Planck-scale remnant would require a full quantum-gravity treatment beyond the present analysis.

In contrast to fully four-dimensional analyses, which are often numerical or state-dependent, the present model provides analytic control of flux, backreaction, entropy flow, and Page-like behavior while remaining conceptually transparent. The effective action encodes evaporation, entropy production, and information transfer within a solvable setting that isolates the dominant s -wave sector. The inclusion of greybody corrections or non-conformal matter, while beyond the exact 2D anomaly framework used here, would provide natural directions for extending the model toward more realistic four-dimensional physics.

B. Future directions

- *Charged and nonsingular black holes in de Sitter.* Extending the present framework to charged (Reissner–Nordström–de Sitter) and regular (e.g., Bardeen or Hayward) geometries, either directly in four dimensions or through their two-dimensional dilaton reductions, would enable a unified treatment of inner and cosmological horizons within the anomaly-induced semiclassical theory. In these cases, the trace anomaly provides a natural mechanism for destabilizing the inner (Cauchy) horizon, potentially enforcing strong cosmic censorship and yielding a fully analytic account of the coupled mass–charge evolution and horizon thermodynamics. For nonsingular geometries, embedding them in a de Sitter background could reveal novel evaporation endpoints, horizon mergers, or long-lived remnants within a controlled semiclassical setting.

- *Entanglement islands and quantum extremal surfaces.* A full QES analysis using the explicit Polyakov field and stress tensor developed here could determine the precise island location and Page time, extending recent island-paradigm results to cosmological spacetimes with multiple horizons.
- *Beyond the conformal anomaly.* Including massive or non-conformal fields, through perturbative or numerical treatments, would test the universality of the anomaly-driven results and connect with realistic matter sectors.
- *Cosmological horizon thermodynamics.* The SdS patch behaves as a finite static universe bounded by two thermal walls. Investigating the thermodynamic properties of the cosmological horizon from the interior, including its heat capacity and response to backreaction, may offer insight relevant to inflationary and late-time cosmology.

In summary, the anomaly-corrected SdS model offers a uniquely controlled setting in which quantum backreaction, nonequilibrium thermodynamics, and information recovery can all be treated analytically. It establishes a foundation for exploring quantum steady states and Page-like behavior in spacetimes with multiple horizons, and provides a benchmark for future extensions to charged, rotating, regular or fully quantum-gravitational systems.

ACKNOWLEDGMENTS

It is a pleasure to thank Lars Aalsma, Paul Davies, Cynthia Keeler, Phillip Levin, Don Page, Marija Tomasevic and Tanmay Vachaspati for useful discussions. This work is supported by the U.S. Department of Energy, Office of High Energy Physics, under Award Number DE-SC0019470.

Email: easson@asu.edu

Appendix A: Exact quadrature reduction and the static momentum constraint

Here we collect the semiclassical field equations following from the localized Polyakov action and reduce them, in the static gauge, to first integrals suitable for quadratures. In a static geometry of the form

$$ds^2 = -f(r) dt^2 + f(r)^{-1} dr^2, \quad (\text{A1})$$

with $X = X(r)$, the off-diagonal semiclassical Einstein equation enforces a vanishing total momentum density, $T_{rt} = 0$. Thus an *exact* flux-carrying solution cannot be strictly static; the nonzero Unruh-dS flux is realized in the quasi-static regime used in the main text (or in a time-dependent ansatz, e.g. Eddington-Finkelstein form), while exact static solutions correspond to zero net flux.

1. Preliminaries in static gauge

We work with the localized action

$$\begin{aligned} S = & \frac{1}{4G_4} \int \sqrt{-g} [XR + 2\tilde{V}(X)] \\ & - \frac{N}{96\pi} \int \sqrt{-g} [(\nabla\psi)^2 + 2\psi R], \end{aligned} \quad (\text{A2})$$

whose variation yields (with $T_{\mu\nu}^{(\text{state})}$ the conserved, traceless state contribution)

$$R + 2\tilde{V}'(X) = 0, \quad (\text{A3})$$

$$\frac{1}{4G_4} (-g_{\mu\nu}\square X + \nabla_\mu \nabla_\nu X - \tilde{V}(X) g_{\mu\nu}) = T_{\mu\nu}^{(\psi)} + T_{\mu\nu}^{(\text{state})}, \quad (\text{A4})$$

$$\square\psi = R, \quad T_{\mu\nu}^{(\psi)} = -\frac{N}{24\pi} \left[\nabla_\mu \nabla_\nu \psi - g_{\mu\nu} \square\psi - \frac{1}{2} \nabla_\mu \psi \nabla_\nu \psi + \frac{1}{4} g_{\mu\nu} (\nabla\psi)^2 \right], \quad (\text{A5})$$

so that $T^\mu_\mu = (N/24\pi)R$ reproduces the conformal anomaly and $T^{(\text{state})\mu}_\mu = 0$. In the static gauge one has $\sqrt{-g} = 1$ and

$$R = -f''(r), \quad \square\Phi = \partial_r(f\Phi'(r)) \quad \text{for any scalar } \Phi(r). \quad (\text{A6})$$

Notation. A prime on f or ψ denotes ∂_r , while a prime on \tilde{V} denotes d/dX .

2. First integrals

From (A5) and (A6),

$$(f\psi')' = R = -f''(r) \Rightarrow f\psi' = -f' + C_\psi, \quad (\text{A7})$$

where C_ψ is an integration constant fixed by horizon regularity (in particular $C_\psi = 0$ for regular future horizons).

Taking the trace of (A4) and using traceless $T^{(\text{state})}$ together with (A3) gives

$$\frac{1}{4G_4}(-\square X - 2\tilde{V}(X)) = \frac{N}{24\pi}R = -\frac{N}{12\pi}\tilde{V}'(X), \quad (\text{A8})$$

which in the gauge (A1) yields the radial ‘‘master’’ equation

$$(fX')' = -2\tilde{V}(X) + \frac{G_4 N}{3\pi}\tilde{V}'(X). \quad (\text{A9})$$

Equations (A3) and (A9), together with one diagonal component of (A4), form a closed system for $f(r), X(r), \psi(r)$. Writing out the nontrivial diagonal components and using (A6) one finds

$$\frac{1}{4G_4} \left[f(fX')' - \frac{1}{2}ff'X' + f\tilde{V}(X) \right] = T_{tt}^{\text{tot}}, \quad (\text{A10})$$

$$\frac{1}{4G_4} \left[X'' + \frac{f'}{2f}X' - f^{-1}(fX')' - f^{-1}\tilde{V}(X) \right] = T_{rr}^{\text{tot}}, \quad (\text{A11})$$

with $T_{\mu\nu}^{\text{tot}} := T_{\mu\nu}^{(\psi)} + T_{\mu\nu}^{(\text{state})}$.

State choice and flux— Stationarity implies Killing-current conservation $\nabla_\mu T^\mu{}_t = 0$, hence $T^r{}_t$ is *radially* constant in the gauge (A1). The numerical value of this constant is fixed by the quantum state through horizon regularity in Kruskal coordinates (e.g. Unruh-dS). In the main text we show that, in the Unruh-dS state, this constant coincides with the anomaly-induced steady flux defined there (see Eqs. (21) and (47)).

3. Static momentum constraint and a no-go for exact static flux

The (r, t) component of Eq. (A4) reads

$$\frac{1}{4G_4} \left(g_{rt} \square X - \nabla_r \nabla_t X - \tilde{V}(X) g_{rt} \right) = T_{rt}^{(\psi)} + T_{rt}^{(\text{state})}. \quad (\text{A12})$$

In a static metric ansatz with $g_{rt} = 0$ and $X = X(r)$, the mixed derivative $\nabla_r \nabla_t X$ vanishes, so the left-hand side of (A12) is identically zero. The off-diagonal field equation then enforces

$$T_{rt}^{(\psi)} + T_{rt}^{(\text{state})} = 0, \quad T^r{}_t = 0. \quad (\text{A13})$$

It is convenient to define $J := -T^r{}_t$ as the flux in the static limit. The momentum constraint (A13) thus requires $J = 0$, showing that no exact static solution of the semiclassical equations (A3)–(A5) can support a nonzero energy flux. Although stationarity implies $\nabla_\mu T^\mu{}_t = 0$ (so $T^r{}_t$ is radially constant), the field equation (A12) fixes that constant to zero in any strictly static geometry. A nonvanishing, radially constant flux $\mathcal{J} \neq 0$ becomes consistent only when strict staticity is relaxed—for instance, in an adiabatic Eddington–Finkelstein gauge where the mass parameter evolves slowly, $M(v)$, with $\dot{M} = -\mathcal{J}(M, \Lambda)$, or more generally in a stationary (nonstatic) ansatz containing g_{vr} or ∂_v terms that balance the (v, r) field equation. This quasi–stationary setting is the framework adopted in the main text.

4. Quadratures and horizon regularity (static, zero-flux case)

In the strictly static case $\mathcal{J} = 0$, regularity on *both* future horizons corresponds to a Hartle–Hawking–dS–type configuration, which for neutral SdS exists only at the Nariai limit. By contrast, the Unruh–dS state (regular on the future horizons but carrying nonzero flux) requires a time-dependent ansatz such as Eddington–Finkelstein form or, equivalently, a quasi-static treatment in which $\dot{M} = -\mathcal{J}(M, \Lambda)$ at leading adiabatic order.

The pair (A3)–(A9) may be viewed as first-order equations for fX' and f' :

$$\begin{aligned} f''(r) &= 2\tilde{V}'(X(r)), \\ (fX')' &= 2\tilde{V}(X) - \frac{G_4 N}{3\pi}\tilde{V}'(X). \end{aligned} \quad (\text{A14})$$

Given a (monotone) branch $X(r)$, the first of (A14) integrates to

$$\begin{aligned} f'(r) &= 2 \int^r ds \tilde{V}'(X(s)) + C_f, \\ f(r) &= 2 \int^r ds \int^s d\bar{s} \tilde{V}'(X(\bar{s})) + C_f r + C_0, \end{aligned} \quad (\text{A15})$$

with constants C_f, C_0 . Equivalently, using X as a radial coordinate ($\frac{d}{dr} = X'(r) \frac{d}{dX}$), (A14) reduces to

$$\begin{aligned}\frac{d}{dX}(f X') &= \frac{2 \tilde{V}(X)}{X'} - \frac{G_4 N}{3\pi} \cdot \frac{\tilde{V}'(X)}{X'}, \\ \frac{d}{dX}(f') &= \frac{2 \tilde{V}'(X)}{X'}.\end{aligned}\tag{A16}$$

These equations are integrable in quadratures once the branch $X(r)$ (or $r(X)$) is chosen. The remaining diagonal equation (A10) (or (A11)) acts as a first integral that fixes (C_ψ, C_f, C_0) in terms of the state data and horizon regularity. Regularity of the renormalized stress tensor on the future horizons \mathcal{H}_b^+ and \mathcal{H}_c^+ fixes the state constants t_u and t_v (Unruh–dS in the main text) and, by horizon regularity, sets $C_\psi = 0$ via (A7). In the strictly static case, (A13) enforces $\mathcal{J} = 0$, i.e. $t_u = t_v$ (no net flux / equilibrium). For neutral SdS a global thermal equilibrium occurs only at the Nariai zero–temperature limit.

Summary—Static solutions necessarily have $\mathcal{J} = 0$; the steady Unruh–de Sitter flux arises only when strict staticity is relaxed, as in the quasi–stationary Eddington–Finkelstein formulation used in the main text.

5. Dimensional-reduction anomaly

The present analysis employs the standard spherically reduced two–dimensional dilaton–gravity action augmented by the Polyakov term, which correctly reproduces the trace anomaly of N conformal matter fields but omits the so–called *dimensional-reduction anomaly*: additional state-dependent terms that arise when integrating out angular modes in the four–dimensional theory. These corrections can modify the quantitative relation between the 4D and 2D fluxes, rescaling the magnitude of \mathcal{J} or shifting the effective dilaton potential. However, they do *not* affect the sign structure of the flux or the inequalities central to our conclusions. The positivity of $\Delta = \kappa_b^2 - \kappa_c^2$, the direction of energy flow $\mathcal{J} \propto \Delta(M)$, and the non–negativity of the generalized entropy production rate $\dot{S}_{\text{gen}} \sim \mathcal{J}(1/T_c - 1/T_b)$ follow purely from geometric relations among the Schwarzschild–de Sitter horizons and thus remain unchanged under any overall normalization of the stress tensor. In this sense, the dimensional–reduction anomaly alters *how fast* evaporation proceeds but not *which way* it goes or whether the generalized second law holds. This line of thinking is further justified by results from the four dimensional case [33].

Appendix B: Adiabatic evolution in Eddington–Finkelstein gauge and the mass–loss law

This appendix complements Appendix A by demonstrating that a nonzero constant flux \mathcal{J} is compatible with the semiclassical equations at leading order in a slow-time (adiabatic) expansion. In advanced Eddington–Finkelstein (EF) coordinates, time dependence enters the mixed (v, r) components of the equations of motion, and the mass-loss relation

$$\frac{dM}{dv} = -\mathcal{J} \quad (\text{B1})$$

follows directly from a covariant Casimir (mass function) balance law. We assume $\partial_v f \ll \kappa f$ and keep $\mathcal{O}(N)$ backreaction from the Polyakov anomaly.

1. EF ansatz and basic identities

To describe flux solutions it is convenient to work in advanced Eddington–Finkelstein (EF) coordinates (v, r) with

$$\begin{aligned} ds^2 &= -f(v, r) dv^2 + 2 dv dr, \\ X &= X(r) \quad (\text{for the Schwarzschild–de Sitter reduction, } X = r^2), \\ \psi &= \psi(v, r), \end{aligned} \quad (\text{B2})$$

where the classical metric function is

$$f_{\text{cl}}(M, \Lambda; r) = 1 - \frac{2M}{r} - \frac{\Lambda}{3} r^2,$$

and we allow the mass parameter $M = M(v)$ to vary slowly, incorporating $\mathcal{O}(N)$ backreaction corrections in f .

Comment on coordinates—In the EF chart the metric is non-diagonal, so its inverse has both $g^{rv} = 1$ and $g^{rr} = f(v, r)$. These components are distinct from those appearing in the diagonal (static) gauge of Eq. (A1); no mixing of coordinate systems occurs. The same function f appears because it represents the redshift factor of the geometry in either chart.

Useful identities in this gauge are

$$\sqrt{-g} = 1, \quad g^{vv} = 0, \quad g^{vr} = g^{rv} = 1, \quad g^{rr} = f, \quad (B3)$$

$$\square\Phi = 2\partial_v\partial_r\Phi + \partial_r(f\partial_r\Phi), \quad (B4)$$

$$R = -\partial_r^2 f(v, r). \quad (B5)$$

The localized Polyakov equation $\square\psi = R$ therefore becomes

$$2\partial_v\psi' + (f\psi')' = -f''(v, r). \quad (B6)$$

Here primes denote ∂_r and we use dots for ∂_v .

2. Mixed Einstein equation and state flux

From the localized action (see Appendix A), the (v, r) component of the semiclassical Einstein equation is

$$\frac{1}{4G_4} \left[\frac{1}{2} f' X' - \partial_r(fX') - \tilde{V}(X) \right] = T_{vr}^{(\psi)} + T_{vr}^{(\text{state})}, \quad (B7)$$

where we have used $\nabla_v\nabla_r X = \frac{1}{2}f'X'$, $g_{vr} = 1$, and $\square X = \partial_r(fX')$.

Taking ∂_v of (B7), and noting that $X'(r)$ and $\tilde{V}(X)$ are v -independent, yields

$$\frac{1}{4G_4} \left[\frac{1}{2} \dot{f}' X' - \partial_r(\dot{f} X') \right] = \partial_v T_{vr}^{(\psi)} + \partial_v T_{vr}^{(\text{state})}. \quad (B8)$$

In the Unruh-dS state, $\partial_v T_{vr}^{(\text{state})} = 0$ (since the flux is stationary). The Polyakov term $\partial_v T_{vr}^{(\psi)}$ is higher order in the adiabatic expansion ($\sim \partial_v^2\psi$ or $\partial_v f'$) and can be neglected at leading order. However, Eq. (B8) by itself does not directly yield a mass-loss law; to obtain one, it is useful to introduce a covariantly conserved quantity, which we do next.

3. Mass function (Casimir) balance and $\dot{M} = -\mathcal{J}$

We now derive the mass-loss law from a covariant conservation identity. Define $Q(X)$ by $Q'(X) = -U(X)$ and $I(X) := e^{-Q(X)}$. The mass function (or dilaton Casimir) is defined by

$$\mathcal{C} = I(X)(\nabla X)^2 + w(X), \quad w'(X) = \tilde{V}(X). \quad (B9)$$

In the presence of matter, the exact balance law reads

$$\nabla_\mu \mathcal{C} = -2G_4 I(X) T_{\mu\nu} \nabla^\nu X. \quad (\text{B10})$$

With $X = X(r)$ in the EF metric (B2), one has $\nabla^\nu X = g^{\nu r} X'$ and $T_{\nu\nu} \nabla^\nu X = X' T^r_\nu$, so

$$\partial_v \mathcal{C} = -2G_4 I(X) X'(r) T^r_\nu. \quad (\text{B11})$$

Identifying $\mathcal{C} = 2G_4 M(v)$ (up to an additive constant) yields the general mass–loss formula

$$\dot{M}(v) = -I(X) X'(r) T^r_\nu. \quad (\text{B12})$$

Frame checks. In the Weyl frame ($U = 0 \Rightarrow I = 1$) with $X = r^2$ we get

$$\dot{M}(v) = -2r T^r_\nu. \quad (\text{B13})$$

In the original SRG frame ($U = 1/(2X) \Rightarrow Q' = -1/(2X)$, $I = e^{-Q} = \sqrt{X} = r$) one has $I(X) X'(r) = r \cdot 2r = 2r^2$, hence

$$\dot{M}(v) = -2r^2 T^r_\nu. \quad (\text{B14})$$

It is convenient to define the EF flux (which is radially conserved at leading adiabatic order)

$$\mathcal{J} := I(X) X'(r) T^r_\nu, \quad (\text{B15})$$

$$\dot{M}(v) = -\mathcal{J}. \quad (\text{B16})$$

In Eddington–Finkelstein gauge, the semiclassical equations therefore admit an adiabatically evolving solution in which the constant Unruh–de Sitter flux \mathcal{J} drives the mass according to Eq. (B16). This derivation explicitly shows how the time-dependent ansatz circumvents the static momentum constraint of Appendix A and provides a covariant foundation for the mass–loss law used in the main text.

Appendix C: Nariai limit in the two–dimensional reduction

In the spherical reduction of four-dimensional Einstein gravity,

$$ds_{(4)}^2 = g_{ab}(x) dx^a dx^b + r^2(x) d\Omega_2^2, \quad (\text{C1})$$

the two-dimensional dilaton field is $X = r^2$. The Schwarzschild–de Sitter (SdS) spacetime possesses two horizons, the black-hole and cosmological horizons (r_b, r_c) , defined by the zeros of

$$\xi(r; M, \Lambda) = 1 - \frac{2M}{r} - \frac{\Lambda r^2}{3}. \quad (\text{C2})$$

The *Nariai limit* corresponds to the extremal configuration in which these horizons coincide,

$$r_b = r_c = r_N = \frac{1}{\sqrt{\Lambda}}, \quad M = M_N = \frac{1}{3\sqrt{\Lambda}}, \quad X_N = r_N^2 = \frac{1}{\Lambda}. \quad (\text{C3})$$

At $r = r_N$ one has

$$\xi(r_N) = 0 = \xi'(r_N), \quad (\text{C4})$$

so that the surface gravities vanish, $\kappa_b = \kappa_c = 0$, and the geometry factorizes as $\text{dS}_2 \times S^2$.

1. Near-horizon scaling and coordinates

To obtain the Nariai metric explicitly, we expand the four-dimensional SdS metric near the degenerate horizon and introduce rescaled coordinates that remain finite as the double root forms. Let ε parameterize the deviation from extremality such that $r_c - r_b \propto \varepsilon$. Define dimensionless near-horizon coordinates

$$r = r_N(1 + \varepsilon y), \quad t = \frac{\tau}{\varepsilon}, \quad (\text{C5})$$

and take the limit $\varepsilon \rightarrow 0$ with (τ, y) held fixed. The variable $y \in (-1, 1)$ is a dimensionless static coordinate on the two-dimensional de Sitter factor, with Killing horizons at $y = \pm 1$, while τ is the corresponding static time. The $1/\varepsilon$ rescaling ensures a nontrivial finite limit since the surface gravity vanishes linearly with ε . Although $t = \tau/\varepsilon$ formally diverges as $\varepsilon \rightarrow 0$, this simply reflects the infinite redshift at the degenerate horizon; the rescaled time τ remains finite and defines the proper static time coordinate of the Nariai patch.

2. Two-dimensional Nariai geometry

Substituting (C5) into the reduced two-dimensional metric $ds_{(2)}^2 = -\xi(r) dt^2 + \xi(r)^{-1} dr^2$ (with $\xi \equiv f$) and expanding to leading order in ε yields

$$ds_{(2)}^2 = \frac{1}{\Lambda} \left[-(1 - y^2) d\tau^2 + \frac{dy^2}{1 - y^2} \right], \quad (\text{C6})$$

which is the static patch of two-dimensional de Sitter space dS_2 with curvature radius $\ell_2 = 1/\sqrt{\Lambda}$. The corresponding Ricci scalar is

$$R^{(2)} = 2\Lambda, \quad (C7)$$

and the Killing horizons of the metric lie at $y = \pm 1$.

At the same time, the dilaton approaches a constant,

$$X = r^2 \longrightarrow X_N = \frac{1}{\Lambda}, \quad (C8)$$

so the internal S^2 factor freezes at radius r_N . The full four-dimensional Nariai geometry is therefore

$$dS_2(\ell_2^2 = 1/\Lambda) \times S^2(r_N^2 = 1/\Lambda). \quad (C9)$$

3. Interpretation in the 2D dilaton theory

In the two-dimensional dilaton-gravity framework, the Nariai configuration corresponds to a *double root* of the Killing function $\xi(X)$,

$$\xi(X_N) = 0 = \xi'(X_N) \iff w'(X_N) = \tilde{V}(X_N) = 0. \quad (C10)$$

At this point, the static patch reaches its degenerate boundary: the black-hole and cosmological horizons coincide, the surface gravity and Hawking temperature vanish, and the two-dimensional metric becomes exactly dS_2 with constant dilaton. This configuration represents the limiting equilibrium state of neutral Schwarzschild-de Sitter spacetime in both the four-dimensional and two-dimensional descriptions.

Appendix D: Curvature scalar and horizon regularity

Here we evaluate the two-dimensional Ricci scalar for the semiclassical backreacted metric and verify its finiteness throughout the static patch, including both the black-hole and cosmological horizons. This provides a direct geometric check that trace-anomaly backreaction preserves smoothness of the metric and does not induce curvature singularities.

1. Ricci scalar in static (or EF) gauge

In the static gauge

$$ds^2 = -f(r) dt^2 + f(r)^{-1} dr^2, \quad (\text{D1})$$

the two-dimensional Ricci scalar is

$$R(r) = -f''(r). \quad (\text{D2})$$

(Equivalently, in the corresponding ingoing Eddington–Finkelstein form $ds^2 = -\xi(r) dv^2 + 2dv dr$, one has $R = -\xi''(r)$, since $f(r) \equiv \xi(r)$ for the static solution.) Using instead the dilaton equation of motion from the localized action,

$$R + 2\tilde{V}'(X) = 0, \quad (\text{D3})$$

and recalling $X = X(r)$ in the semiclassical solution, one finds the equivalent form

$$R(r) = -2\tilde{V}'(X(r)), \quad (\text{D4})$$

which holds exactly. Thus the Ricci scalar depends on backreaction only through the quantum-corrected dilaton profile $X(r)$, determined by the master equation, Eq. A9.

Since $X = r^2 \in [X_b, X_c]$ with $X_b > 0$ and $\tilde{V}'(X)$ smooth on this interval, the backreacted Ricci scalar is finite throughout the static patch.

2. Finiteness at the horizons

Let $r = r_h$ be a (nondegenerate) Killing horizon, $f(r_h) = 0$ with $f'(r_h) = 2\kappa_h \neq 0$. Expanding near r_h ,

$$f(r) = 2\kappa_h(r - r_h) + \frac{1}{2}f''(r_h)(r - r_h)^2 + \mathcal{O}((r - r_h)^3), \quad (\text{D5})$$

the curvature is

$$R(r_h) = -f''(r_h) = -2\tilde{V}'(X_h), \quad X_h := X(r_h), \quad (\text{D6})$$

which is finite provided $X(r)$ remains smooth at the horizon—guaranteed by the regularity conditions imposed when solving the semiclassical field equations.

Degenerate limit—In the Nariai limit $\kappa_h \rightarrow 0$ the linear term vanishes, but the analysis proceeds with the next term in the expansion; $R = -f''(r)$ remains finite.

3. Classical limit and backreaction corrections

Since the anomaly-induced backreaction enters linearly in the Polyakov coefficient, we may write

$$R(r) = R_{\text{cl}}(r) + \delta R(r), \quad \delta R(r) = \mathcal{O}(N), \quad (\text{D7})$$

with $R_{\text{cl}}(r) = -f_{\text{cl}}''(r)$ for classical Schwarzschild–de Sitter. Equivalently, using the exact relation

$$R(r) = -2\tilde{V}'(X(r)), \quad (\text{D8})$$

the Ricci scalar depends on backreaction only through the quantum-corrected dilaton profile $X(r)$ determined by the master equation (A9). Because $X(r)$ is smooth on $[r_b, r_c]$ (in the regular Unruh–de Sitter state) and $\tilde{V}'(X)$ is smooth on $[X_b, X_c]$, $\delta R(r)$ is finite and $R(r) \rightarrow R_{\text{cl}}(r)$ smoothly as $N \rightarrow 0$. Thus the two-dimensional Ricci scalar is regular throughout the static patch, including both horizons; its deviation from the classical value is controlled by the trace anomaly and remains finite, confirming the smoothness of the semiclassical solution and the validity of the expansion.

- [1] Jacob D. Bekenstein, “Black holes and entropy,” *Phys. Rev. D* **7**, 2333–2346 (1973).
- [2] Jacob D. Bekenstein, “Generalized second law of thermodynamics in black hole physics,” *Phys. Rev. D* **9**, 3292–3300 (1974).
- [3] James M. Bardeen, B. Carter, and S. W. Hawking, “The Four laws of black hole mechanics,” *Commun. Math. Phys.* **31**, 161–170 (1973).
- [4] S. W. Hawking, “Black hole explosions,” *Nature* **248**, 30–31 (1974).
- [5] S. W. Hawking, “Particle Creation by Black Holes,” *Commun. Math. Phys.* **43**, 199–220 (1975), [Erratum: *Commun.Math.Phys.* 46, 206 (1976)].
- [6] Alexander M. Polyakov, “Quantum Geometry of Bosonic Strings,” *Phys. Lett. B* **103**, 207–210 (1981).
- [7] S. M. Christensen and S. A. Fulling, “Trace Anomalies and the Hawking Effect,” *Phys. Rev. D* **15**, 2088–2104 (1977).
- [8] P. C. W. Davies, S. A. Fulling, and W. G. Unruh, “Energy Momentum Tensor Near an Evaporating Black Hole,” *Phys. Rev. D* **13**, 2720–2723 (1976).

- [9] Curtis G. Callan, Jr., Steven B. Giddings, Jeffrey A. Harvey, and Andrew Strominger, “Evanescence black holes,” *Phys. Rev. D* **45**, R1005 (1992), arXiv:hep-th/9111056.
- [10] Jorge G. Russo, Leonard Susskind, and Larus Thorlacius, “The Endpoint of Hawking radiation,” *Phys. Rev. D* **46**, 3444–3449 (1992), arXiv:hep-th/9206070.
- [11] A. Fabbri and J. Navarro-Salas, *Modeling black hole evaporation* (World Scientific, Singapore, 2005).
- [12] Jorge G. Russo, Leonard Susskind, and Larus Thorlacius, “Black hole evaporation in (1+1)-dimensions,” *Phys. Lett. B* **292**, 13–18 (1992), arXiv:hep-th/9201074.
- [13] Raphael Bousso and Stephen W. Hawking, “Trace anomaly of dilaton coupled scalars in two-dimensions,” *Phys. Rev. D* **56**, 7788–7791 (1997), arXiv:hep-th/9705236.
- [14] R. Balbinot and A. Fabbri, “Hawking radiation by effective two-dimensional theories,” *Phys. Rev. D* **59**, 044031 (1999), arXiv:hep-th/9807123.
- [15] Raphael Bousso and Stephen W. Hawking, “(Anti)evaporation of Schwarzschild-de Sitter black holes,” *Phys. Rev. D* **57**, 2436–2442 (1998), arXiv:hep-th/9709224.
- [16] Panagiota Kanti and John March-Russell, “Calculable corrections to brane black hole decay. 2. Greybody factors for spin 1/2 and 1,” *Phys. Rev. D* **67**, 104019 (2003), arXiv:hep-ph/0212199.
- [17] Shijun Yoshida and Toshifumi Futamase, “Numerical analysis of quasinormal modes in nearly extremal Schwarzschild-de Sitter space-times,” *Phys. Rev. D* **69**, 064025 (2004), arXiv:gr-qc/0308077.
- [18] Ruth Gregory, Ian G. Moss, Naritaka Oshita, and Sam Patrick, “Black hole evaporation in de Sitter space,” *Class. Quant. Grav.* **38**, 185005 (2021), arXiv:2103.09862 [gr-qc].
- [19] Ana Alonso-Serrano, Marek Liška, and Michał Piotrak, “Semi-classical spacetime thermodynamics,” (2025), arXiv:2509.05052 [hep-th].
- [20] Tom Banks and M. O’Loughlin, “Nonsingular Lagrangians for two-dimensional black holes,” *Phys. Rev. D* **48**, 698–706 (1993), arXiv:hep-th/9212136.
- [21] M. Trodden, Viatcheslav F. Mukhanov, and Robert H. Brandenberger, “A Nonsingular two-dimensional black hole,” *Phys. Lett. B* **316**, 483–487 (1993), arXiv:hep-th/9305111.
- [22] Aleksandar Bogojevic and Dejan Stojkovic, “A Nonsingular black hole,” *Phys. Rev. D* **61**, 084011 (2000), arXiv:gr-qc/9804070.
- [23] Damien A. Easson and Robert H. Brandenberger, “Universe generation from black hole interiors,” *JHEP* **06**, 024 (2001), arXiv:hep-th/0103019.

[24] Damien A. Easson, “Hawking radiation of nonsingular black holes in two-dimensions,” *JHEP* **02**, 037 (2003), arXiv:hep-th/0210016.

[25] Damien A. Easson, “Nonsingular Schwarzschild–de Sitter black hole,” *Class. Quant. Grav.* **35**, 235005 (2018), arXiv:1712.09455 [hep-th].

[26] Valeri P. Frolov and Andrei Zelnikov, “Two-dimensional black holes in the limiting curvature theory of gravity,” *JHEP* **08**, 154 (2021), arXiv:2105.12808 [hep-th].

[27] Paul C. W. Davies, Damien A. Easson, and Phillip B. Levin, “Nonsingular black holes as dark matter,” *Phys. Rev. D* **111**, 103512 (2025), arXiv:2410.21577 [hep-th].

[28] Robert B. Mann, A. Shiekh, and L. Tarasov, “Classical and Quantum Properties of Two-dimensional Black Holes,” *Nucl. Phys. B* **341**, 134–154 (1990).

[29] Thomas Klosch and Thomas Strobl, “Classical and quantum gravity in (1+1)-Dimensions. Part 1: A Unifying approach,” *Class. Quant. Grav.* **13**, 965–984 (1996), [Erratum: *Class.Quant.Grav.* **14**, 825 (1997)], arXiv:gr-qc/9508020.

[30] D. Grumiller, W. Kummer, and D. V. Vassilevich, “Dilaton gravity in two-dimensions,” *Phys. Rept.* **369**, 327–430 (2002), arXiv:hep-th/0204253.

[31] Richard Tolman and Paul Ehrenfest, “Temperature Equilibrium in a Static Gravitational Field,” *Phys. Rev.* **36**, 1791–1798 (1930).

[32] Damien A. Easson, “Quantum enforcement of strong cosmic censorship,” (2025), arXiv:2511.05656 [gr-qc].

[33] Stefan Hollands, Robert M. Wald, and Jochen Zahn, “Quantum instability of the Cauchy horizon in Reissner–Nordström–deSitter spacetime,” *Class. Quant. Grav.* **37**, 115009 (2020), arXiv:1912.06047 [gr-qc].

[34] Hidekazu Nariai, “On a New Cosmological Solution of Einstein’s Field Equations of Gravitation,” *Gen. Rel. Grav.* **31**, 963–971 (1999).

[35] José P. S. Lemos and Oleg B. Zaslavskii, “Hot spaces with positive cosmological constant in the canonical ensemble: de Sitter solution, Schwarzschild–de Sitter black hole, and Nariai universe,” *Phys. Rev. D* **109**, 084016 (2024), arXiv:2402.05166 [hep-th].

[36] Kota Numajiri, Kazumasa Okabayashi, and Shinji Mukohyama, “Boulware vacuum vs regularity: Thoughts on anomaly-induced effective action,” *Phys. Rev. D* **111**, 085024 (2025), arXiv:2411.12617 [gr-qc].

[37] Ahmed Almheiri, Netta Engelhardt, Donald Marolf, and Henry Maxfield, “The entropy of bulk quantum fields and the entanglement wedge of an evaporating black hole,” *JHEP* **12**, 063 (2019), arXiv:1905.08762 [hep-th].

[38] Geoffrey Penington, “Entanglement Wedge Reconstruction and the Information Paradox,” *JHEP* **09**, 002 (2020), arXiv:1905.08255 [hep-th].

[39] Ahmed Almheiri, Thomas Hartman, Juan Maldacena, Edgar Shaghoulian, and Amirhossein Tajdini, “The entropy of Hawking radiation,” *Rev. Mod. Phys.* **93**, 035002 (2021), arXiv:2006.06872 [hep-th].

[40] Hao Geng, Andreas Karch, Carlos Perez-Pardavila, Lisa Randall, Marcos Riojas, Sanjit Shashi, and Merna Youssef, “Constraining braneworlds with entanglement entropy,” *SciPost Phys.* **15**, 199 (2023), arXiv:2306.15672 [hep-th].

[41] Daniel Harlow and Hirosi Ooguri, “Symmetries in quantum field theory and quantum gravity,” *Commun. Math. Phys.* **383**, 1669–1804 (2021), arXiv:1810.05338 [hep-th].

[42] William Donnelly and Laurent Freidel, “Local subsystems in gauge theory and gravity,” *JHEP* **09**, 102 (2016), arXiv:1601.04744 [hep-th].

[43] William Donnelly and Aron C. Wall, “Entanglement entropy of electromagnetic edge modes,” *Phys. Rev. Lett.* **114**, 111603 (2015), arXiv:1412.1895 [hep-th].

[44] Venkatesa Chandrasekaran, Roberto Longo, Geoff Penington, and Edward Witten, “An algebra of observables for de Sitter space,” *JHEP* **02**, 082 (2023), arXiv:2206.10780 [hep-th].

[45] Hao Geng, Yasunori Nomura, and Hao-Yu Sun, “Information paradox and its resolution in de Sitter holography,” *Phys. Rev. D* **103**, 126004 (2021), arXiv:2103.07477 [hep-th].